AMERICAN SOCIETY FOR MICROBIOLOGY | Journal of Virology

Mouse Hepatitis Virus Infection Induces a Toll-Like Receptor 2-Dependent Activation of Inflammatory Functions in Liver Sinusoidal Endothelial Cells during Acute Hepatitis

Christian Bleau,[a] Aveline Filliol,[b] Michel Samson,[b] Lucie Lamontagne[a]

Département des Sciences Biologiques, Université du Québec à Montréal, Montreal, Canada[a]; U.1085 Inserm, Institut de Recherche en Santé-Environnement-Travail, Université de Rennes 1, Rennes, France[b]

ABSTRACT

Under physiological conditions, the liver sinusoidal endothelial cells (LSECs) mediate hepatic immune tolerance toward self or foreign antigens through constitutive expression of anti-inflammatory mediators. However, upon viral infection or Toll-like receptor 2 (TLR2) activation, LSECs can achieve proinflammatory functions, but their role in hepatic inflammation during acute viral hepatitis is unknown. Using the highly virulent mouse hepatitis virus type 3 (MHV3) and the attenuated variants 51.6-MHV3 and YAC-MHV3, exhibiting lower tropism for LSECs, we investigated *in vivo* and *in vitro* the consequence of LSEC infection on their proinflammatory profiles and the aggravation of acute hepatitis process. *In vivo* infection with virulent MHV3, in comparison to attenuated strains, resulted in fulminant hepatitis associated with higher hepatic viral load, tissue necrosis, and levels of inflammatory mediators and earlier recruitment of inflammatory cells. Such hepatic inflammatory disorders correlated with disturbed production of interleukin-10 (IL-10) and vascular factors by LSECs. We next showed *in vitro* that infection of LSECs by the virulent MHV3 strain altered their production of anti-inflammatory cytokines and promoted higher release of proinflammatory and procoagulant factors and earlier cell damage than infection by attenuated strains. This higher replication and proinflammatory activation in LSECs by the virulent MHV3 strain was associated with a specific activation of TLR2 signaling by the virus. We provide evidence that TLR2 activation of LSCEs by MHV3 is an aggravating factor of hepatic inflammation and correlates with the severity of hepatitis. Taken together, these results indicate that preservation of the immunotolerant properties of LSECs during acute viral hepatitis is imperative in order to limit hepatic inflammation and damage.

IMPORTANCE

Viral hepatitis B and C infections are serious health problems affecting over 350 million and 170 million people worldwide, respectively. It has been suggested that a balance between protection and liver damage mediated by the host's immune response during the acute phase of infection would be determinant in hepatitis outcome. Thus, it appears crucial to identify the factors that predispose in exacerbating liver inflammation to limit hepatocyte injury. Liver sinusoidal endothelial cells (LSECs) can express both anti- and proinflammatory functions, but their role in acute viral hepatitis has never been investigated. Using mouse hepatitis virus (MHV) infections as animal models of viral hepatitis, we report for the first time that *in vitro* and *in vivo* infection of LSECs by the pathogenic MHV3 serotype leads to a reversion of their intrinsic anti-inflammatory phenotype toward a proinflammatory profile as well to as disorders in vascular factors, correlating with the severity of hepatitis. These results highlight a new virus-promoted mechanism of exacerbation of liver inflammatory response during acute hepatitis.

Under physiological conditions, the liver adopts mechanisms of immune tolerance toward innocuous gut-derived food and microbial antigens (such as lipopolysaccharide [LPS]) to prevent undesired inflammatory responses. The induction of tolerance in the liver is mediated by several resident hepatic cell types, such as the endothelial cells (ECs) lining the hepatic sinusoids (liver sinusoidal endothelial cells [LSECs]), the Kupffer cells (KCs), and to a lesser extent the hepatocytes (1). However, the tolerizing and anti-inflammatory functions of LSECs were recently shown to be more efficient than those of KCs (2). Given their anatomical situation, LSECs are first in contact with portal-delivered antigens and thus act as a sieving barrier in expressing highly efficient sentinel and scavenger functions that contribute to clearance of microbial products (3). They also tightly control blood-parenchyma exchanges via a dynamic regulation of the sinusoidal blood flow in releasing vasoactive factors such as NO (reviewed in reference 4). LSECs play a major role in liver tolerance in displaying a restricted Toll-like receptor (TLR)-mediated activation profile to microbial products (5, 6) and producing large amounts of anti-inflammatory cytokines, such as transforming growth factor β (TGF-β) and interleukin-10 (IL-10) (7, 8). However, upon viral infection or stimulation by TLR1/2 ligands, LSECs can switch toward an inflammatory and immunogenic state and induce recruitment of leukocytes and virus-specific $CD8^+$ T cell immunity (5, 9). The role of LSECs in inflammatory

Received 1 June 2016 **Accepted** 23 July 2016

Accepted manuscript posted online 3 August 2016

Citation Bleau C, Filliol A, Samson M, Lamontagne L. 2016. Mouse hepatitis virus infection induces a Toll-like receptor 2-dependent activation of inflammatory functions in liver sinusoidal endothelial cells during acute hepatitis. J Virol 90:9096–9113. doi:10.1128/JVI.01069-16.

Editor: S. Perlman, University of Iowa

Address correspondence to Lucie Lamontagne, lamontagne.lucie@uqam.ca.

liver diseases is poorly understood, but as these cells can express both anti- and proinflammatory functions, they could act as either moderators or exacerbators of liver inflammation.

Hepatitis B virus (HBV) and hepatitis C virus (HCV) infections are serious health problems affecting over 350 million and 170 million people worldwide, respectively (10). Most liver damage in HBV/HCV infections is attributed primarily to an exuberant immunopathological response triggered by viral infection rather than direct injury caused by viral replication (11, 12). It has been suggested that the balance between protection and liver damage mediated by the host's immune response during the acute phase of infection would be critical in the outcome of hepatitis (13). Evidence suggests that an exacerbated hepatic inflammatory response during acute infection may predispose to the development of a fulminant hepatic failure characterized by extensive hepatocellular dysfunctions and high mortality (14). The role of LSECs in viral hepatitis is largely unknown, and data are somewhat contradictory. Indeed, LSECs were suggested to contribute to the clearance of HCV and HBV from the bloodstream (15, 16) and to control HCV replication (17) or instead to promote its transmission to hepatocytes by acting as a viral reservoir (18). A few data suggest that LSECs may also participate in hepatic inflammation, since fibrinogen-like factor 2 (Fgl2), promoting vascular thrombosis and hepatic inflammation, and the proinflammatory alarmin IL-33, both produced by LSECs, are upregulated in acute or chronic hepatitis (19–22). A better understanding of the role of LSECs during the acute phase of viral hepatitis may help to identify new mechanisms that predispose to inflammation-driven hepatocyte injury and liver failure.

Mouse hepatitis virus type 3 (MHV3), belonging to the coronavirus family, is a relevant murine model to unravel the role of LSECs in acute viral hepatitis. MHV3 infects LSECs, hepatocytes, Kupffer cells (KCs), and Ito cells, all of which express the carcinoembryonic antigen 1a (CEACAM1a) viral receptor, and induces fulminant hepatitis leading to death of susceptible C57BL/6 mice within 3 to 4 days (23–25). LSECs are thought to play an important role in the resistance of A/J mice to MHV3 infection by controlling viral replication and delaying the transmission of the viral progeny to hepatocytes (26). Previous studies have reported early structural and vascular disorders in LSECs during MHV3 infection in susceptible C57BL/6 mice. Indeed, a reduced number of fenestrations in liver sinusoids and a correlation between the fulminance of hepatitis and the induction of Fgl2 in LSECs have been described (27, 28). We have also shown that MHV3 infection was associated with early release of IL-33 by LSECs (29) and a reduction in the intrahepatic levels of immunosuppressive IL-10, prostaglandin E_2 (PGE_2), and TGF-β cytokines, suggesting virus-induced disturbances in LSEC-mediated liver tolerance (30). Several attenuated MHV3 variants, such as the 51.6- and YAC-MHV3 viruses, have been *in vitro* generated to study the role of specific hepatic cell types in the hepatitis process. Compared to the parental MHV3, the major difference of the 51.6-MHV3 variant is its inefficiency of replication in LSECs (24). This difference is reflected by induction of milder hepatitis and higher hepatic levels of IL-10 and TGF-β (30). The YAC-MHV3 variant, showing lower tropism for LSECs and macrophages, induces a subclinical hepatitis characterized by few perivascular inflammatory foci (31) and higher induction of anti-inflammatory cytokines in the liver than with 51.6-MHV3 (30). The absence of vascular thrombosis combined with efficient recruitment of mononuclear cells favors hepatic clearance of YAC-MHV3 and full recovery of infected mice within 15 days (32). These improved clinical outcomes in mice infected by the attenuated variants support the hypothesis that preservation of the structural and functional integrity of LSECs may be one determining factor in the severity of hepatitis.

In this study, we report that robust infection of LSECs by the highly virulent MHV3, in contrast to the attenuated 51.6- and YAC-MHV3 variants, promotes disturbances in their anti-inflammatory functions and secretion of vascular factors, resulting in high release of inflammatory mediators and procoagulant Fgl2 simultaneously with decrease in NO and IL-10 levels. Such MHV3-induced LSEC disorders correlated *in vivo* with higher hepatic inflammation, damage, and viral replication as well as disturbances in leukocyte recruitment in mice infected by MHV3. We provide evidence that higher infection and proinflammatory activation of LSECs by MHV3 was related to a specific viral induction of TLR2 signaling. The aggravating role for TLR2 in hepatic inflammation and LSEC disorders was confirmed in MHV3-infected TLR2 knockout (KO) mice, in which hepatic damage, the pro- versus anti-inflammatory cytokine ratio, and LSEC-derived IL-10 production were significantly improved.

MATERIALS AND METHODS

Mice. Female C57BL/6 (Charles River, St-Constant, Quebec, Canada) and TLR2 KO (C57BL/6-129 $Tlr^{tm/Kir}$/J; Jackson Laboratory, Bar Harbor, ME) mice were housed in a HEPA-filtered air environment. All experiments were conducted with mice between 8 and 10 weeks of age in compliance with the regulations of the Animal Committee of the University of Quebec in Montreal (CIPA).

Viruses. MHV3 is a cloned pathogenic substrain isolated from the livers of infected DBA2 mice. MHV3 induces a rapid mortality in C57BL/6 mice within 3 to 4 days postinfection (p.i.) (23). The escape mutant 51.6-MHV3 was selected from the pathogenic MHV3 virus cultured into L2 cells in the presence of S protein-specific A51 monoclonal antibodies (24). This variant induces a delayed mortality (5 to 9 days p.i.) and expresses low tropism for LSECs but retains ability to infect Kupffer cells (KCs) (24). The nonpathogenic YAC-MHV3 variant is a cloned substrain produced in persistently infected YAC-1 cells, showing lower ability to replicate in LSECs and macrophages. Compared to the attenuated 51.6-MHV3 strain, this variant causes no mortality and induces efficient recruitment of innate immune cells, allowing viral clearance from the liver within 2 weeks p.i. (31). All viruses were passaged fewer than three times onto L2 cells, and their pathogenic properties were assessed routinely.

Isolation and purification of LSECs. Mice were euthanized, and the portal vein was isolated and injected with 3 ml of Hanks balanced salt solution (HBSS)–10 nM HEPES followed by 3 ml of digestion buffer consisting of 0.2% (wt/vol) collagenase A in HBSS–10 nM HEPES (Sigma-Aldrich, St. Louis, MO). The liver was then excised, injected several times with digestion buffer, and dissociated by a 30-min incubation in 10 ml of digestion buffer at 37°C on a shaking plate (200 rpm). The resulting cell suspension was passed through sterile 70-μm and 40-μm nylon mesh filters successively (Falcon; BD Biosciences, Mississauga, Ontario, Canada) and centrifuged at 400 × *g* for 10 min. The cell pellet was resuspended in 3 ml of RPMI 1640, layered at the top of a discontinuous 50%/25% Percoll gradient (Sigma-Aldrich), and centrifuged at 800 × *g* for 20 min without brakes. The interphase between the two density cushions, containing enriched nonparenchymal cells, was collected and washed with phosphate-buffered saline (PBS). LSECs were then purified using the positive-selection phycoerythrin (PE) kit (Stemcell, Vancouver, Canada) with an anti-CD146 monoclonal antibody, a specific marker of endothelial cells in liver (33), according to the manufacturer's procedure. LSEC purity was analyzed by cytometry before each experiment and reached over 90%.

TABLE 1 Primers used for quantitative reverse transcription-PCR

Gene	Forward primer	Reverse primer
HPRT	5′-GAAAGACTTGCTCGAGATGTCATG-3′	5′-CACACAGAGGGCCACAATGT-3′
IL-6	5′-TCGGAGGCTTAATTACACATGTTC-3′	5′-TGCCATTGCACAACTCTTTTCT-3′
TNF-α	5′-TCCCAGGTTCTCTTCAAGGGA-3′	5′-GGTGAGGAGCACGTAGTCGG-3′
CCL2	5′-GCAGCAGGTGTCCCAAAGAA-3′	5′-GGTCAGCACAGACCTCTCTCTTG-3′
CXCL10	5′-GGCCATAGGGAAGCTTGAAAT-3′	5′-TCGTGGCAATGATCTCAACAC-3′
ICAM-1	5′-GTCCGCTGTGCTTTGAGAACT-3′	5′-CGGAAACGAATACACGGTGAT-3′
TLR3	5′-TGGGCTGAAGTGGACAAATCT-3′	5′-TGCCGACATCATGGAGGTT-3′
CAV-1	5′-GCGCACACCAAGGAGATTG-3′	5′-CACGTCGTCGTTGAGATGCT-3′
TLR7	5′-CAGTGAACTCTGGCCGTTGA-3′	5′-CAAGCCGGTTGTTGGAGAA-3′
MHV-N	5′-TGGAAGGTCTGCACCTGCTA-3′	5′-TTTGGCCCACGGGATTG-3′
RIG-I	5′-GCCAGAGTGTCAGAATCTCAGTCAG-3′	5′-GAGAACACAGTTGCCTGCTGCTCA-3′
MDA-5	5′-GCCCTCTCCTTCCTCTGAGACT-3′	5′-GCTGGAGGAGGGTCAGCAA-3′
IL-33	5′-GCTGCGTCTGTTGACACATTG-3′	5′-GGGAGGCAGGAGACTGTGTTAA-3′
Fgl2	5′-CGTTGTGGTCAACAGTTTGGA-3′	5′-GATGTTGAACCGGCTGTGACT-3′
CXCL1	5′-CCGAAGTCATAGCCACACTCAA-3′	5′-CAAGGGAGCTTCAGGGTCAA-3′
IL-10	5′-GATGCCCCAGGCAGAGAA-3′	5′-CACCCAGGGAATTCAAATGC-3′
TGF-β	5′-AGCGCTCACTGCTCTTGTGA-3′	5′-GCTGATCCCGTTGATTTCCA-3′

***In vivo* viral infections.** Groups of 6 or 7 wild-type (WT) C57BL/6 or TLR2 KO mice were intraperitoneally (i.p.) infected with 10^3 50% tissue culture infective doses ($TCID_{50}$) of MHV3, 51.6-MHV3, or YAC-MHV3. Mock-infected mice received a similar volume of PBS. Mice were sacrificed by CO_2 anoxia at 24, 48, or 72 h postinfection (p.i.). Liver and blood samples were collected and frozen for further analyses.

Histopathological and immunohistochemical (IHC) analyses and determination of transaminase levels. The histopathological analysis of liver was done by hematoxylin-eosin-safranin staining. Determination of serum alanine transaminase (ALT) and aspartate transaminase (AST) was performed according to the IFCC primary reference procedures using an Olympus AU2700 Autoanalyser (Olympus Optical, Tokyo, Japan). Immunolocalization of IL-33 and caveolin-1 (CAV-1) was performed on liver sections fixed in paraformaldehyde and embedded in paraffin incubated with primary goat anti-mouse IL-33 (R&D Systems Inc., Minneapolis, MN) or rabbit anti-mouse CAV-1 (LSBio, Seattle, WA) for 1 h in a Ventana automated machine (Ventana Medical Systems, Inc., Tucson, AZ) and secondary horseradish peroxidase (HRP)-conjugated rabbit anti-goat antibody (Dako, Markham, Ontario, Canada) or OmniMap anti-rabbit–HRP (RUO) for 16 min. Double-immunofluorescence stainings of IL-10 or IL-33 and CAV-1 were conducted on liver cryosections fixed in paraformaldehyde and incubated overnight with primary goat anti-mouse IL-10 (R&D Systems Inc., Minneapolis, MN) or primary goat anti-mouse IL-33 (R&D Systems) and rabbit anti-mouse CAV-1 (LSBio) and then with DyLight-649 anti-goat Cy3 anti-rabbit secondary antibodies (Jackson ImmunoResearch, West Grove, PA) and Hoechst counterstain (Invitrogen, Ontario, Canada). Slides were mounted (mounting medium; Invitrogen, Ontario, Canada), imaged with a Nikon Eclipse Ni-E Z1 microscope, and analyzed using SpotAdvance software.

Virus titration. Frozen liver samples from mice infected with MHV for 24 or 72 h were weighed and homogenized in cold PBS. The suspension was then centrifuged at 13,000 rpm for 30 min and analyzed for viral detection. Viral titration was also performed on LSEC culture supernatants. Liver suspension and cell culture supernatants were 10-fold serially diluted and tested for viral presence on L2 cells cultured in 96-well plates. Cytopathic effects (CPE), characterized by the occurrence of large syncytia and cell lysis, were recorded at 72 h p.i., and virus titers were determined according to the Reed-Muench method and expressed as $\log_{10}$ $TCID_{50}$.

***In vitro* viral infections.** Freshly isolated LSECs were seeded in 24-well plates at a density of 7.5×10^5 cells/ml in RPMI 1640 supplemented with 10% fetal calf serum (FCS) and antibiotics (Wysent, St-Bruno, Quebec, Canada). Cells were then infected with infectious MHV3, YAC-MHV3, or 51.6-MHV3 at a multiplicity of infection (MOI) of 0.1 and incubated at 37°C under 5% CO_2 for 24 to 72 h depending on the experiment. Cell culture supernatants were collected for enzyme-linked immunosorbent assays (ELISAs), and total RNA was extracted for quantitative reverse transcription-PCR (qRT-PCR) analysis.

siRNA transfection. LSECs were seeded in 24-well plates at 60 000 cells/ml and transfected with 25 nM small interfering RNA (siRNA) Flexitude premix (Qiagen, Cambridge, MA) targeting TLR2 mRNA (target sequence, CTCGTTCTCCAGCATTTAAA) and with the AllStars negative-control siRNA as a nonsilencing transfection control for 36 h prior to infection for 24 h.

RNA isolation and qRT-PCR. RNA from *in vitro*-infected LSECs was extracted using the NucleoSpin RNA II kit (Macherey-Nagel, Bethlehem, PA) according to the manufacturer's procedure. Total RNA from frozen liver samples was extracted using TRIzol reagent (Invitrogen, Burlington, Ontario, Canada), and, residual genomic DNA was removed with the Turbo DNA-free kit (Ambion, Austin, TX). One microgram of RNA was reverse transcribed into cDNA using a high-capacity cDNA reverse transcription kit (Applied Biosystems, Foster City, CA). Real-time PCR amplification was carried out on 25 ng cDNA using the HotStart-IT SYBR green qPCR master mix (USB Corporation, Cleveland, OH) on an ABI 7300 system (Applied Biosystems). The primer sets used are listed in Table 1. Threshold cycle (C_T) values were collected and used for $\Delta\Delta C_T$ analysis. The gene expression was normalized to that of hypoxanthine phosphoribosyltransferase (HPRT) as an endogenous control and expressed as a ratio to gene expression in mock-infected mice livers or control (uninfected) LSECs in *in vitro* experiments (level arbitrarily taken as 1). The specificity of the PCR products was confirmed by melting curve analyses, and all qPCR assays were run in duplicate.

ELISA and nitric oxide assay. Frozen liver samples were weighed and homogenized in NP-40 lysis buffer (Invitrogen) with a protease inhibitor cocktail (Sigma-Aldrich, St. Louis, MO) and 1 mM phenylmethylsulfonyl fluoride (PMSF) for protein extraction. The liver suspension was kept on ice for 30 min and centrifuged for 10 min at 13,000 rpm. Determination of IL-6 and tumor necrosis factor alpha (TNF-α) (BD BioSciences, San Jose, CA), CXCL10 and CCL2 (eBioscience, San Diego, CA), and CXCL1 and IL-33 (R&D Systems, Minneapolis, MN) in liver lysates and/or LSEC culture supernatants was carried out by ELISAs. Levels of nitric oxide (NO) were quantified using the Griess reagent assay (Invitrogen) according to the manufacturer's procedure.

Cytofluorometric studies. Livers were perfused with PBS through the portal vein to remove blood cell contamination prior to dissection. Liver tissues were then homogenized, and hepatocytes were removed by sedi-

mentation. Inflammatory cells were enriched using 35% Percoll gradient (Sigma-Aldrich), and red blood cells were lysed with a Tris-buffered ammonium chloride solution. One million (10^6) leukocytes were incubated with anti-CD16/32 antibodies (BD Biosciences) to block nonspecific binding. Cells were incubated with optimal dilutions of anti-CD3–V500, anti-Gr1–V450, anti-CD11b–PE-Cy7, anti-CD19–allophycocyanin (APC), anti-CD4–fluorescein isothiocyanate (FITC), anti-NK1.1–peridinin chlorophyll protein (PerCP)-Cy-5.5, and anti-CD8–APC-Cy7 antibodies (BD Biosciences) and fixed in PBS containing 2% FCS, 0.01 M sodium azide, and 2% formaldehyde. Stained cells were analyzed on a FACSAria II flow cytometer using BD FACS Diva software (BD Bioscience), and the data were processed using CXP software (Beckman Coulter, Mississauga, Ontario, Canada). Dead cells and doublet cells were excluded on the basis of forward scatter (FSC) and side scatter (SCC), and analyses were performed on 10,000 events recorded. Myeloid cells, gated by high side scatter, were assessed for CD11b and Gr1 to enumerate macrophages ($CD11b^+$ $Gr1^{inter}$) and neutrophils ($CD11b^+$ $Gr1^{high}$). Lymphoid cells were gated according to FSC/SCC and first assessed for NK1.1 and CD3 expression to discriminate NK from NK-T cells. $CD3^+$ $NK1.1^-$ T cells were further gated to allow determination of $CD4^+$ and $CD8^+$ subpopulations. B lymphocytes were determined by $CD19^+$ $CD3^-$ expression.

Statistical analyses. Data are expressed as mean ± standard error of the mean. Statistical analyses for *in vitro* studies were performed with Student's *t* test comparing uninfected (control) to virus-infected cells or virulent to attenuated MHV3 infections. Multiple-group analyses were conducted for *in vivo* studies, and data obtained by qPCR, ELISA, and viral titration were evaluated by one-way analysis of variance (ANOVA) with *post hoc* Tukey test using PASW Statistics software (PASW version 18; IBM SPSS Inc., Chicago, IL). *P* values of ≤0.05 were considered significant.

RESULTS

Lower tropism of attenuated MHV3 variants for LSECs is associated with less severe damage and less viral replication in the liver. Previous studies have shown that acute infections by the attenuated 51.6- and YAC-MHV3 variants resulted in milder or subclinical hepatitis, respectively, in comparison to the fulminant hepatitis induced by the parental virulent MHV3 strain (24, 31). We first aimed to compare the evolution of damage, inflammatory infiltrates, and viral replication in the livers of mice infected by virulent and attenuated MHV3 strains. C57BL/6 mice were i.p. infected with either MHV3 or attenuated viruses for 24 to 72 h, and blood and liver samples were collected for clinical, histopathology, and viral titer analyses. Liver histopathology for virulent MHV3-infected mice showed inflammatory foci surrounding necrotic cells at 24 h and 48 h p.i.; these disappeared at 72 h p.i., while hepatocyte necrosis became extensive (Fig. 1A and B). Infection with 51.6-MHV3 revealed a delayed occurrence of inflammatory foci at 48 h p.i. with barely detectable hepatic damage, while YAC-MHV3 induced few small inflammatory infiltrates with no observable hepatic necrosis areas even at 72 h p.i. (Fig. 1A and B). Extensive hepatic damage in virulent MHV3-infected mice correlated with high levels of blood ALT and AST at 72 h p.i. ($P \leq 0.001$) (Fig. 1C and D) and sooner and higher viral replication than in mice infected with the attenuated 51.6- and YAC-MHV3 variants ($P \leq 0.01$ to 0.001) (Fig. 1E and F).

Attenuated MHV3 strains induce lower Fgl2, CAV-1, and IL-33 expression in the liver than virulent MHV3. Vascular and structural disorders in LSECs were reported in viral hepatitis, correlating with hepatic damage (19, 27, 29). Indeed, previous studies have demonstrated that induction of Fgl2, a prothrombinase expressed by LSECs and promoting vascular thrombosis and hepatic inflammation, correlated with MHV3-induced fulminant hepatitis (28). Moreover, a direct association between capillarization (lack of fenestrations) of LSECs in livers from HCV-infected patients and overexpression of caveolin-1 (CAV-1), a key component of LSEC fenestrations, was recently reported (34). To verify whether the lower severity of hepatitis induced by the attenuated MHV3 strains was associated with less dysfunction in LSECs, mRNA levels for CAV-1 and Fgl2 in livers from all infected groups of mice were quantified by qRT-PCR. Intrahepatic expression of CAV-1 in MHV3- and 51.6-MHV3-infected mice was also localized by immunohistochemical staining. As shown in Fig. 2A, greater increases of CAV-1 mRNA levels were observed at 48 h p.i. in the livers of MHV3-infected mice while less or no induction was noted in 51.6- and YAC-MHV3-infected mice ($P \leq 0.001$ and 0.05, respectively). Immunolocalization of CAV-1 revealed specific expression in LSECs and confirmed higher induction in the livers of MHV3-infected mice than in those of 51.6-MHV3-infected mice (Fig. 2B). Fgl2 gene expression increased as soon as 24 h p.i. in mice infected with MHV3, while it was delayed and lower in 51.6-MHV3 infection and not induced in YAC-MHV3-infected mice ($P \leq 0.05$ to 0.001) (Fig. 2C). In addition, Fgl2 mRNA reached higher levels in the livers of mice infected with virulent MHV3 than in those infected with attenuated viruses ($P \leq 0.001$).

We have recently reported that MHV3 infection was associated with early release of IL-33, an alarmin secreted mainly by injured LSECs (29). We aimed to verify whether lower tropism of attenuated MHV3 strains for LSECs may be associated with lower expression of IL-33. To test this hypothesis, mRNA expression, production, and localization of IL-33 in livers from MHV3- and 51.6-MHV3-infected groups of mice were assessed by qRT-PCR, ELISA, and IHC, respectively. As shown in Fig. 2D and E, gene expression and release of IL-33 increased only in the livers of MHV3-infected mice ($P \leq 0.001$), while IL-33 was not induced or was inhibited in mice infected with 51.6- or YAC-MHV3 ($P \leq 0.05$ to 0.01). IHC stainings indicated that expression of IL-33 was induced only in the liver of MHV3-infected mice and was localized mostly in LSECs and to a lesser extent in hepatocyte nuclei (Fig. 2F). Induction of IL-33 in LSECs in livers from MHV3-infected mice at 48 h p.i. and to a lesser extent at 72 h p.i. was confirmed by double immunostaining of IL-33 and caveolin-1 (Fig. 2G).

Virulent MHV3 infection leads to an imbalance of pro- over anti-inflammatory mediators in the liver, in contrast to infection by attenuated MHV3 strains. Given the crucial role of LSECs in the control of liver inflammation through production of anti-inflammatory cytokines, we presumed that dysfunction of LSECs in MHV3-infected mice may favor the induction of a proinflammatory state in the liver. To verify this hypothesis, levels of anti-inflammatory cytokines (IL-10 and TGF-β) and proinflammatory cytokines (IL-6 and TNF-α) and chemokines (CCL2, CXCL1, and CXCL10) were assayed by qRT-PCR (from 24 to 72 h p.i.) and ELISA (72 h p.i.) in the livers of all groups of infected mice. As indicated in Fig. 3IA and B, mRNA expression levels and production of IL-10 were markedly increased in the livers of 51.6-MHV3- and YAC-MHV3-infected mice compared to MHV3-infected mice ($P \leq 0.05$ to 0.001). To a lesser extent, TGF-β mRNA and production levels were also more induced in the livers of 51.6-MHV3-infected mice, especially at 24 and 48 h p.i. ($P \leq 0.05$ to 0.001) (Fig. 3IC and D). To determine whether IL-10 induction in the livers of 51.6-MHV3-infected mice occurred in endothelial cells (ECs), immunohistochemistry staining using specific anti-

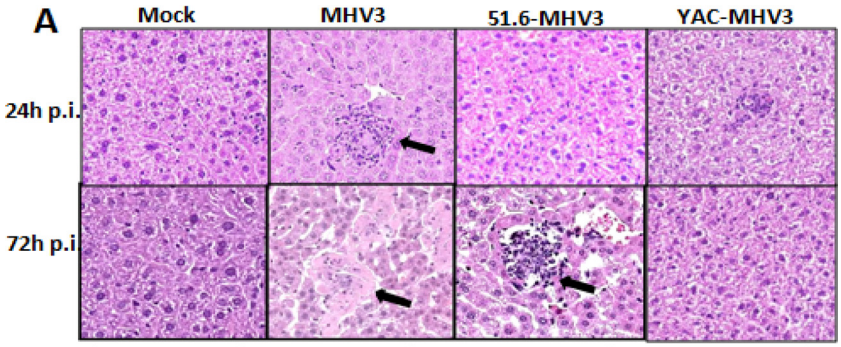

B

Virus	Time p.i. (hrs)	Inflammatory foci	Hepatic necrosis foci
MHV3	24	++	-
	48	++	++
	72	+	++++
51.6-MHV3	24	-	-
	48	+	+
	72	++	+
YAC-MHV3	24	+	-
	48	+	-
	72	+	-

+ (scarce foci); ++ (10% of hepatic tissue); +++ (20-30% of hepatic tissue); ++++ (up to 40% of hepatic tissue)

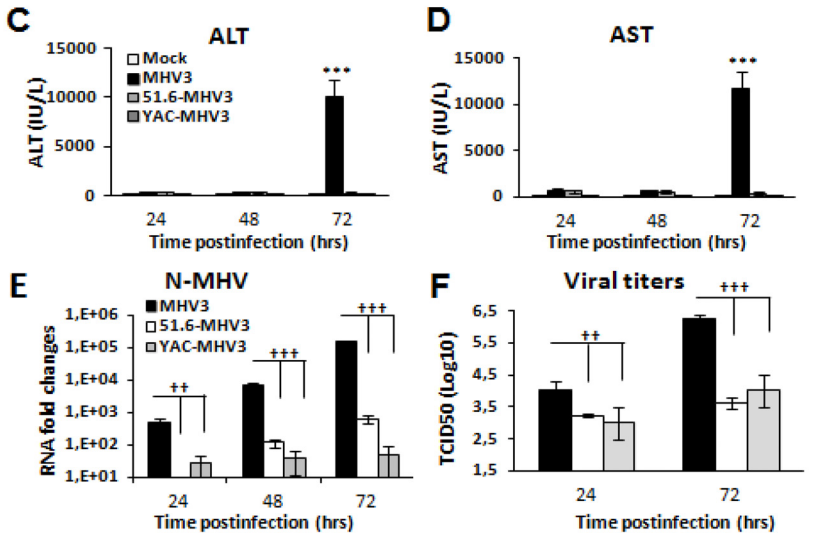

FIG 1 Hepatic damage and viral replication in highly hepatotropic MHV3- and attenuated 51.6- and YAC-MHV3-infected mice. Groups of 5 or 6 C57BL/6 mice were intraperitoneally infected with 1,000 $TCID_{50}$ of MHV3, 51.6-MHV3, or YAC-MHV3. (A) Histopathological analysis was conducted on livers from mock- and virus-infected mice from each group at 24 and 72 h p.i. Inflammatory and necrotic foci are indicated by arrows. (B) Summary of occurrence of necrotic and inflammatory foci in livers from infected mice at 24, 48, and 72 h p.i. (C and D) ALT (C) and AST (D) activities were assayed in serum samples from mock- and virus-infected mice at 24, 48, and 72 h p.i. ***, $P < 0.001$ (compared with mock-infected mice). (E and F) MHV3 replication in livers from each group of infected mice was determined by analysis of the nucleoprotein (NP) RNA expression at 24, 48, and 72 h p.i. by qRT-PCR (E) and by viral titration ($TCID_{50}$) (F) at 24 h and 72 h p.i. Values represent fold change in gene expression relative to that in mock-infected mice after normalization to HPRT expression. Values are means and standard errors of the means. ††, $P < 0.01$; †††, $P < 0.001$ (compared with MHV3-infected mice).

bodies to IL-10 and CAV-1 (an EC marker) was conducted on liver sections. In comparison to results for mock-infected mice, IL-10 expression in livers from 51.6-MHV3-infected mice was induced in the parenchyma and in venous and sinusoidal ECs, whereas the occurrence and intensity of IL-10 staining were weaker in MHV3-infected mice (Fig. 3II).

On the other hand, intrahepatic IL-6 and TNF-α mRNA expression and production levels were more upregulated in MHV3-infected mice than in 51.6- or YAC-MHV3-infected mice ($P \leq 0.05$ to 0.001) (Fig. 3IE to H). Along the same line, chemokine CXCL1, CCL2, and CXCL10 transcription and production levels increased throughout infection by MHV3 but were delayed or dramatically reduced in 51.6- or YAC-MHV3-infected mice ($P \leq 0.05$ to 0.001) (Fig. 3IIIA to F).

Virulent MHV3 induces higher expression of TLRs and helicases in the liver than attenuated MHV3 strains. Induction of the

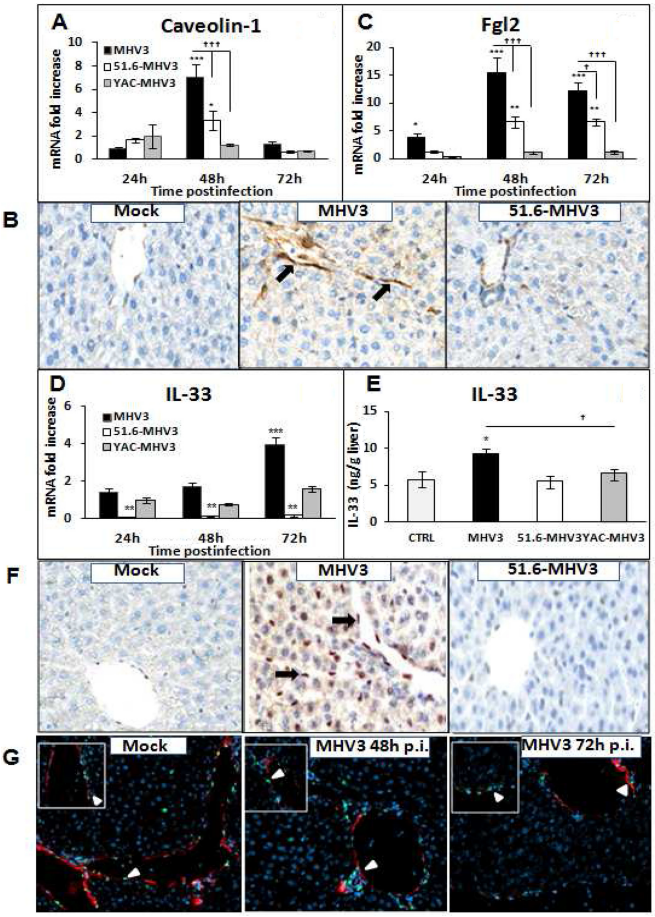

FIG 2 Gene expression and production of caveolin-1, Fgl2, and IL-33 in the livers of MHV3-, 51.6-MHV3-, and YAC-MHV3-infected mice. Groups of 5 or 6 C57BL/6 (WT) mice were intraperitoneally infected with 1,000 $TCID_{50}$ of MHV3, 51.6-MHV3, and YAC-MHV3. At 24, 48, or 72 h p.i., livers were collected from mock- and virus-infected mice of each group. (A, C, and D) mRNA expression for caveolin-1 (A), Fgl2 (C), and IL-33 (D) genes was evaluated by qRT-PCR. Values represent fold change in gene expression relative to that in mock-infected mice (arbitrarily taken as 1) after normalization to HPRT expression. (B and F) *In situ* expression of caveolin-1 (B) and IL-33 (F) in livers from mock-, MHV3-, and 51.6-MHV3-infected mice at 48 h p.i. was determined by immunohistochemistry. Caveolin-1- and IL-33-positive cells are indicated by arrows. (E) Levels of production of IL-33 at 72 h p.i. in the liver of each mouse were quantified by ELISA. (G) Immunolocalization of IL-33 in LSECs was confirmed by double immunostaining of IL-33 (green) and CAV-1 (red) in livers from mock- and MHV3-infected mice at 48 and 72 h p.i. Cell nuclei were counterstained with Hoechst (blue). Values are means and standard errors of the means. *, $P < 0.05$; **, $P < 0.01$; ***, $P < 0.001$ (compared with mock-infected mice). †, $P < 0.05$; ††, $P < 0.01$; †††, $P < 0.001$ (compared with MHV3-infected mice).

inflammatory response during viral infection is triggered upon activation of pattern recognition receptors (PRRs), such as TLRs and helicases, by viral products. Several studies have reported increased TLR expression in viral hepatitis, correlating with liver inflammation (reviewed in reference 17). We explored the hypothesis that higher release of inflammatory mediators in MHV3 infection may be related to increased expression of TLRs or helicases in the liver. Thus, the kinetics of surface TLR2 and -4, endosomal TLR3 and -7, and helicase RIG-1 and MDA-5 gene expression in the livers of infected mice were compared by qRT-PCR from 24 to 72 h p.i. As shown in Fig. 4A, TLR2 expression steadily increased over the course of infection with MHV3, while its induction was drastically reduced in mice infected with the attenuated variants ($P \leq 0.01$ to 0.001). Expression levels of the TLR3, TLR4, RIG-1, and MDA-5 genes were increased equally or more during MHV3 infection than during 51.6- or YAC-MHV3 infection, albeit markedly less so than TLR2 ($P \leq 0.05$ to 0.001) (Fig. 4B, C, E, and F), whereas levels of TLR7 were unaffected by any of the viruses (Fig. 4D).

These data suggest that higher levels of inflammatory mediators in the livers of MHV3-infected mice may be associated with preferential and higher induction of PRRs, especially TLR2, by the virulent MHV3.

The hepatic proinflammatory state in virulent MHV3-infected mice leads to rapid but transient intrahepatic recruitment of inflammatory cells and decreases of B, CD4, and CD8 lymphocyte subsets. LSECs are responsible for the recruitment and transmigration of leukocytes during liver inflammation (35). We postulated that higher production of chemokines in the livers of MHV3-infected mice induced higher recruitment of inflammatory cells than in mice infected with attenuated virus strains. This hypothesis was supported by higher occurrence of inflammatory infiltrates in the livers of MHV3-infected mice at 24 h p.i. (Fig. 1A). To determine leukocyte subsets recruited into the liver, intrahepatic mononuclear cells were isolated at 24 and 48 h p.i. from all groups of mice and immunolabeled, and the percentages of NK-T ($NK1.1^+$ $CD3^+$) and NK ($NK1.1^+$ $CD3^-$) cells, neutrophils ($CD11b^{hi}$ $Gr1^{hi}$), macrophages ($CD11b^+$ $Gr1^{int}$), B cells ($CD19^+$), and T cells ($CD8^+$ and $CD4^+$) were analyzed by cytofluorometry and compared to those in cells from mock-infected mice. As shown in Fig. 5IA, the percentages of NK-T cells transiently decreased in the livers of MHV3-infected mice ($P \leq 0.001$), differently from what was seen in livers from 51.6- and YAC-MHV3 infected mice ($P \leq 0.05$ to 0.01). NK cell percentages increased more in MHV3- than in 51.6-MHV3-infected mice, while they decreased in YAC-MHV3-infected mice ($P \leq 0.05$ to 0.001) (Fig. 5IB). Neutrophils, however, were recruited earlier and to higher levels into the livers of MHV3- than into those of 51.6- and YAC-MHV3-infected mice ($P \leq 0.05$ and 0.001, respectively) (Fig. 5IC). Percentages of intrahepatic macrophages increased more in MHV3-infected mice ($P \leq 0.05$ to 0.001) (Fig. 5ID). Regarding lymphocyte subsets, B and $CD4^+$ cell percentages decreased more strongly in the livers of MHV3-infected mice ($P \leq 0.05$ and 0.001, respectively) (Fig. 5IE and F), while $CD8^+$ cells were reduced more by 51.6- or YAC-MHV3 infection ($P \leq 0.05$ to 0.001) (Fig. 5IG).

Since a substantial decrease in the total number of isolated intrahepatic cells was noted over infection time with MHV3 only, the analysis of absolute numbers of each cell subset rather than the relative percentages better reflects the recruitment of inflammatory cells. Cell numbers were then determined, using the percentage of each subset with respect to the total number of isolated cells in the livers of the mice. As shown in Fig. 5IIA and B, NK-T cells decreased only in the livers of MHV3-infected mice ($P \leq 0.01$ and 0.001), while total NK cells were not altered in all infected groups. The number of neutrophils, however, earlier but transiently increased at 24 h p.i. in MHV3-infected mice, while they were delayed or recruited less in livers from 51.6- and YAC-MHV3-infected mice, respectively, compared to MHV3 infection ($P \leq 0.05$ to 0.001) (Fig. 5IIC). In contrast to what was observed with per-

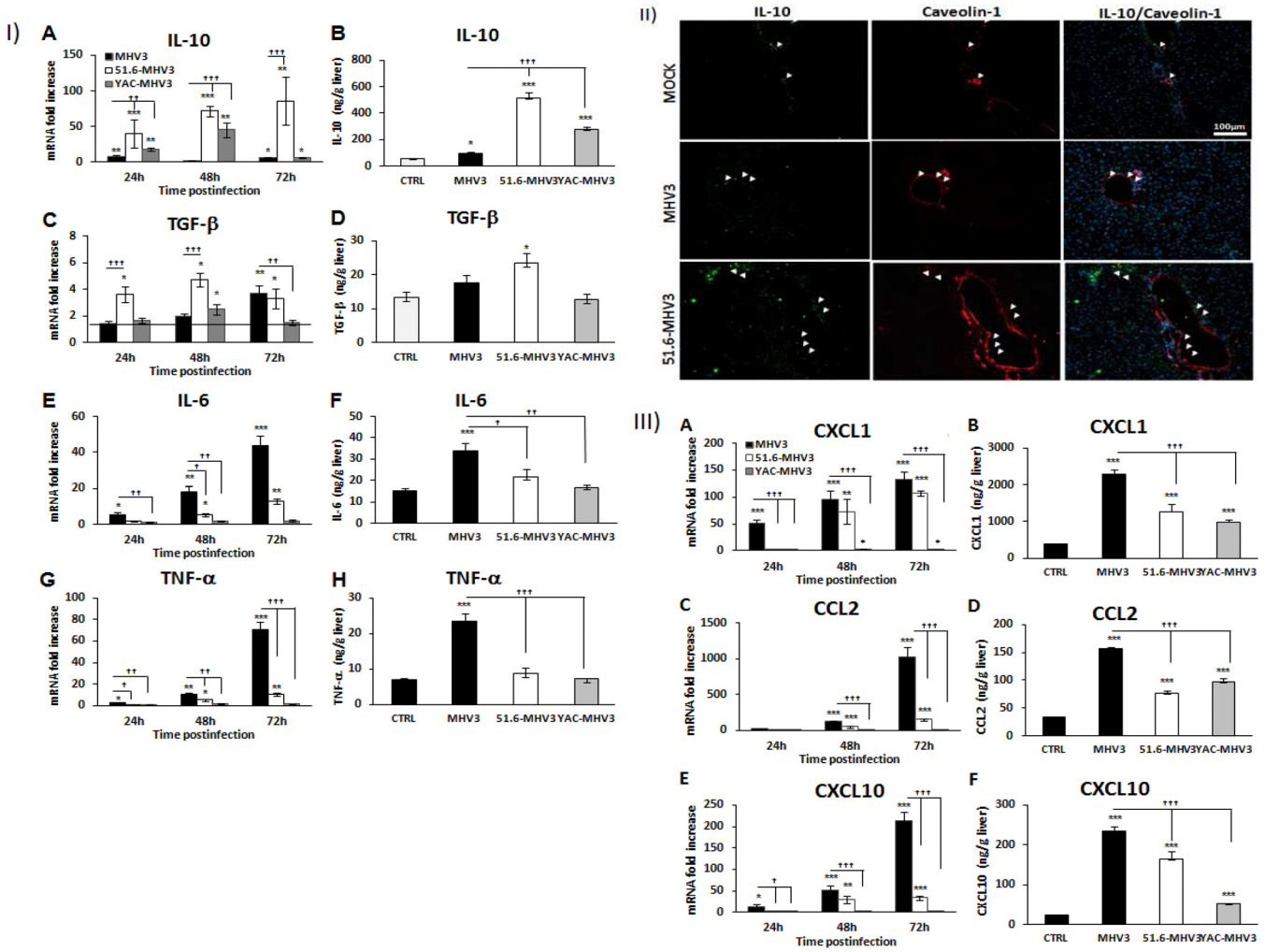

FIG 3 Gene expression and production of IL-10, TGF-β, IL-6, TNF-α, CXCL1, CCL2, and CXCL10 in the livers of MHV3-, 51.6-MHV3-, and YAC-MHV3-infected mice. Groups of 5 or 6 C57BL/6 mice were intraperitoneally infected with 1,000 $TCID_{50}$ of MHV3, 51.6-MHV3, and YAC-MHV3. At 24, 48, or 72 h p.i., livers were collected from mock- and virus-infected mice of each group. (I) Fold changes in mRNAs of IL-10 (A), TGF-β (C), IL-6 (E), and TNF-α (G) were analyzed by qRT-PCR. Values represent fold change in gene expression relative to those in mock-infected mice (arbitrarily taken as 1) after normalization to HPRT expression. Production levels of IL-10 (B), TGF-β (D), IL-6 (F), and TNF-α (H) at 72 h p.i. in the liver of each mouse were quantified by ELISA. (II) *In situ* expression of IL-10 and caveolin-1 was assayed by immunohistochemistry in livers of mock-, MHV3-, and 51.6-MHV3-infected mice at 48 h p.i. (arrows show IL-10- and caveolin-1-expressing endothelial cells). (III) Fold changes in mRNAs of CXCL1 (A), CCL2 (C), and CXCL10 (E) were analyzed by qRT-PCR. Values represent fold change in gene expression relative to that in mock-infected mice (arbitrarily taken as 1) after normalization to HPRT expression. Production levels of CXCL1 (B), CCL2 (D), and CXCL10 (F) at 72 h p.i. in the liver of each mouse were quantified by ELISA. Values are means and standard errors of the means. *, $P < 0.05$; **, $P < 0.01$; ***, $P < 0.001$ (compared with mock-infected mice). †, $P < 0.05$; ††, $P < 0.01$; †††, $P < 0.001$ (compared with MHV3-infected mice).

centages, the numbers of intrahepatic macrophages increased in the livers of mice infected with the attenuated YAC- and 51.6-MHV3 strains ($P \leq 0.01$ and 0.001) but not in those infected with MHV3, but such increases were not statistically significant compared to MHV3 infection (Fig. 5IID). The numbers of B and T (CD4 and CD8) cells were also dramatically impaired over the course of infection by MHV3 but were less or not altered by 51.6- or YAC-MHV3 infections or transiently increased at 24 h p.i. in YAC-MHV3-infected mice ($P \leq 0.05$ to 0.001) (Fig. 5IIE and G).

Permissivity of LSECs to MHV3 strains correlates with virulence. We next attempted to characterize the effect of virulent and attenuated MHV3 infection on the functional and structural integrity of LSECs *in vitro*. LSECs were isolated from the livers of C57BL/6 mice and purified by Percoll gradients followed by immunomagnetism using anti-CD146 antibodies. As shown in Fig. 6A, 87 to 91% of isolated cells expressed the endothelial markers CD146, CD54 (ICAM-1), and CD31 (PECAM-1) but not the macrophage marker F4/80. Isolated LSECs were then infected by the MHV3 strains, and viral replication as well as CPE were monitored from 24 to 120 h p.i. The CPE in LSECs were characterized by cell lysis and rounded cells instead of typical MHV-induced giant syncytial cells (usually observed in L2 cells) and occurred sooner in virulent MHV3-infected culture, as cells were totally lysed by 72 h p.i. In contrast, CPE in cells infected by attenuated strains were delayed to 72 h p.i. and increased up to 120 h p.i. (Fig. 6B) ($P \leq 0.001$ compared with MHV3-infected cells). Infectious viruses in supernatants from MHV3-infected LSECs were

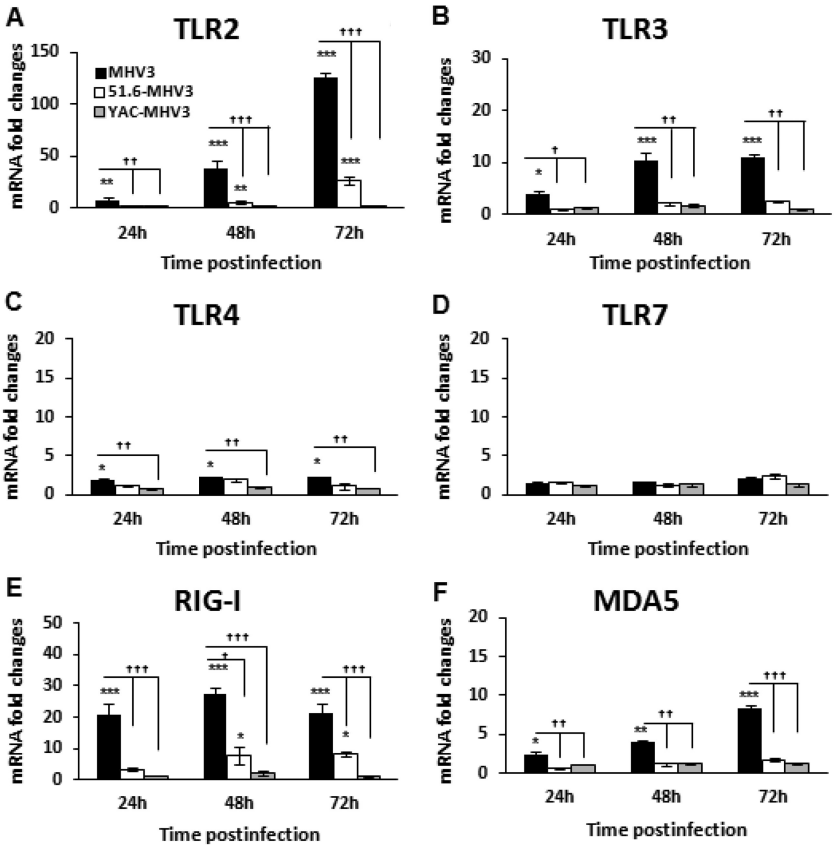

FIG 4 Gene expression of TLR2, -3, -4, and -7 and helicases RIG-I and MDA5 in the livers of MHV3-, 51.6-MHV3-, and YAC-MHV3-infected mice. Groups of 5 or 6 C57BL/6 (WT) mice were intraperitoneally infected with 1,000 $TCID_{50}$ of MHV3, 51.6-MHV3, and YAC-MHV3. At 24, 48, or 72 h p.i., livers were collected from mock- and virus-infected mice of each group. mRNA expression for the TLR2 (A), TLR3 (B), TLR4 (C), TLR7 (D), RIG-I (E), and MDA5 (F) genes was evaluated by qRT-PCR. Values represent fold change in gene expression relative to that in mock-infected mice (arbitrarily taken as 1) after normalization to HPRT expression. Values are means and standard errors of the means. *, $P < 0.05$; **, $P < 0.01$; ***, $P < 0.001$ (compared with mock-infected mice). †, $P < 0.05$; ††, $P < 0.01$; †††, $P < 0.001$ (compared with MHV3-infected mice).

detected at 48 h p.i. and then started to decrease as cell damage became extensive, whereas titers of 51.6- and YAC-MHV3 were detected only after 96 or 120 h p.i. (Fig. 6C) ($P \leq 0.001$ compared with MHV3-infected cells).

Virulent, but not attenuated, strain MHV3 induces Fgl2, IL-33, and caveolin-1 expression and alters NO production by LSECs. To confirm that attenuated MHV3 variants, in contrast to MHV3 virus, do not disturb LSEC integrity and vascular factors, as observed *in vivo*, the expression levels of the alarmin IL-33 and the prothrombinase Fgl2 in infected LSECs were evaluated. As expected and as shown in Fig. 7A to C, gene expression and release of IL-33 increased throughout infection only in MHV3-infected cells ($P \leq 0.05$ to 0.001), while Fgl2 expression was upregulated at 48 h p.i. only in MHV3-infected cells ($P \leq 0.05$ to 0.001). Lower levels of Fgl2 mRNA at 72 h p.i. ($P \leq 0.05$) reflected total cell lysis in MHV3-infected LSECs.

MHV3 replication was already shown to be controlled *in vitro* by nitric oxide (NO) (36). Since LSECs constitutively release NO, a vasodilator factor regulating sinusoidal blood flow (37), we examined whether higher replication of MHV3 in LSECs may result from a defect in NO production by quantifying NO levels in culture supernatants. As shown in Fig. 7D, release of NO was reduced only in MHV3-infected cells and not in 51.6-MHV3- or YAC-MHV3-infected cells ($P \leq 0.01$) (Fig. 7B). Since NO production was reported to be negatively regulated by CAV-1 through inhibition of endothelial nitric oxide synthase (eNOS) activity (38), we investigated whether NO alteration by MHV3 infection was associated with upregulation of CAV-1 expression in infected LSECs, as seen in the livers of MHV3-infected mice. In agreement with our *in vivo* observations, the CAV-1 mRNA expression level increased only in MHV3-infected LSECs at 24 and 48 h p.i. (Fig. 7E) ($P \leq 0.05$ to 0.001).

Virulent MHV3, in contrast to attenuated strains, promotes LSEC conversion to a proinflammatory profile. MHV3-infected mice exhibited a higher inflammatory response in the liver than mice infected by attenuated strains, suggesting a defect in the control of inflammation by LSECs. LSECs were already reported to produce IL-6 upon infection by mouse cytomegalovirus (MCMV) (5), indicating a possible switch from an anti- to a proinflammatory phenotype once infected. We thus speculated that LSECs infected by MHV3, in comparison to attenuated strains, may adopt a preponderant proinflammatory profile. To address this, mRNA expression and production levels of anti-inflammatory (IL-10 and TGF-β) and proinflammatory (IL-6 and TNF-α) cytokines produced by infected LSECs were determined by qRT-PCR and ELISAs. As shown in Fig. 8IA and B, IL-10 mRNA expression and

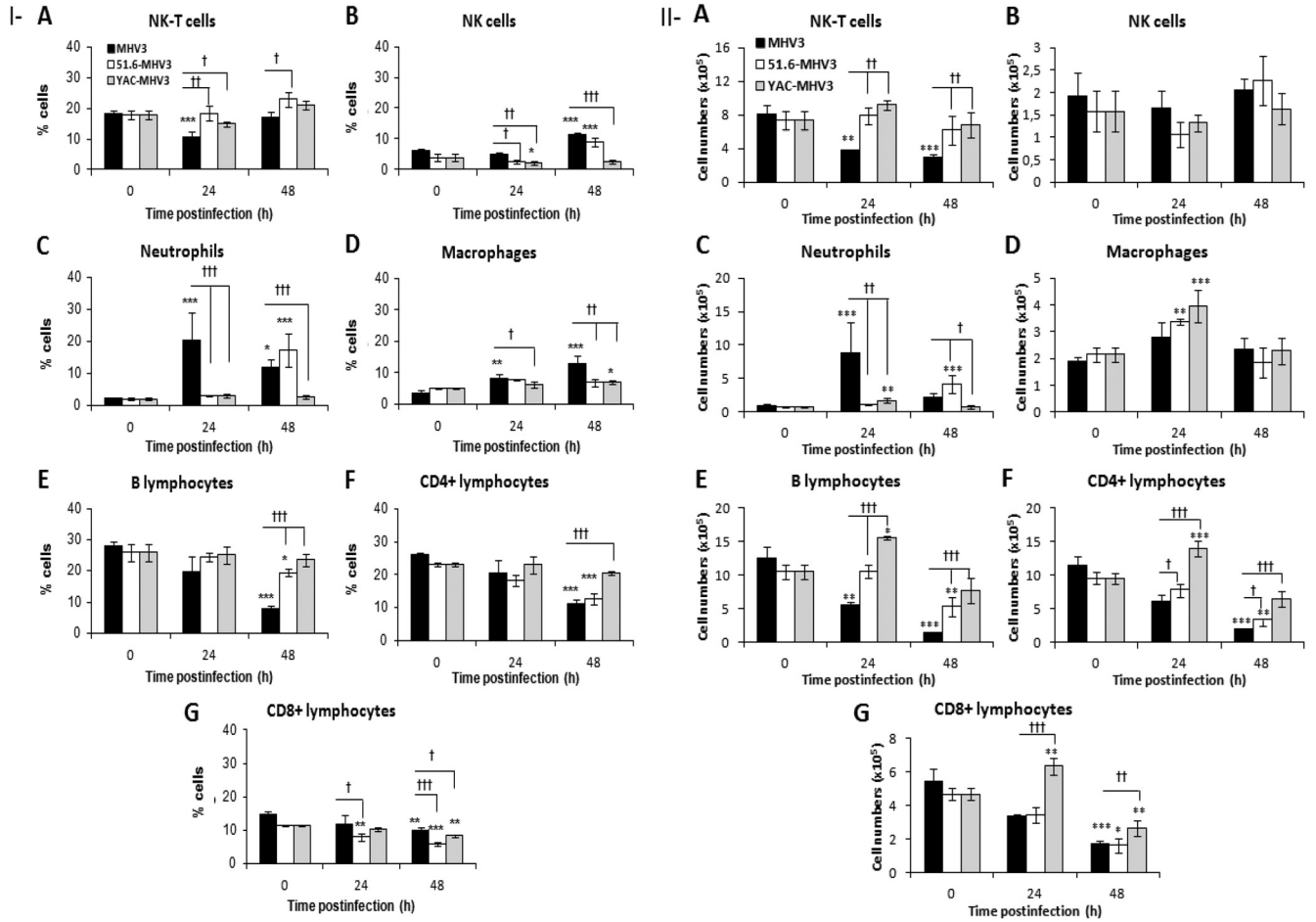

FIG 5 Percentages and numbers of intrahepatic mononuclear cell subsets in livers from MHV3-, 51.6-MHV3-, and YAC-MHV3-infected mice. Intrahepatic mononuclear cells were isolated from groups of 5 or 6 mock-infected or MHV3-, 51.6-MHV3-, or YAC-MHV3-infected C57BL/6 mice at 24 and 48 h p.i., immunolabeled with NK1.1, CD3, Gr1, CD11b, CD19, CD4, and CD8 monoclonal antibodies, and analyzed by cytofluorometry. (I) Percentages of NK-T cells ($NK1.1^+$ $CD3^+$) (A), NK cells ($NK1.1^+$ CD3) (B), neutrophils ($Gr1^{hi}$ $CD11b^{hi}$) (C), macrophages ($Gr1^+$ $CD11b^{int}$) (D), B lymphocytes ($CD19^+$) (E), CD4 cells ($CD3^+$ $CD4^+$) (F), and CD8 cells ($CD3^+$ $CD8^+$) (G) were evaluated in livers from each group of infected mice. (II) Absolute numbers for each cell subset (calculated by using respective percentages reported with respect to the total number of isolated mononuclear cells) were similarly recorded in livers of respective groups. Values are means and standard errors of the means. *, $P < 0.05$; **, $P < 0.01$; ***, $P < 0.001$ (compared with mock-infected mice). †, $P < 0.05$; ††, $P < 0.01$; †††, $P < 0.001$ (compared with MHV3-infected mice).

production slightly increased at 24 h p.i. in MHV3-infected LSECs but decreased thereafter below the basal level in uninfected cells ($P \leq 0.05$ and 0.001). Consistent with the upregulation of IL-10 in the livers of mice infected with attenuated MHV3 strains, IL-10 levels increased rapidly or progressively higher in 51.6-MHV3- and YAC-MHV3-infected LSECs than in MHV3-infected LSECs up to 72 h p.i. ($P \leq 0.05$ to 0.001). TGF-β expression, however, was not induced or was slightly induced in cells infected by the attenuated strains ($P \leq 0.05$) but was less inhibited in attenuated-virus-infected cells than in virulent MHV3-infected cells ($P \leq 0.05$ and 0.01) (Fig. 8IC and D). These results suggest that MHV3 infection suppresses the anti-inflammatory function of LSECs whereas attenuated strains promote it.

TNF-α mRNA levels, however, transiently increased only in MHV3-infected LSECs at 24 h p.i. ($P \leq 0.01$) (Fig. 3IE) and were completely inhibited at 72 h p.i. by all MHV3 strains ($P \leq 0.01$). The amounts of TNF-α released in supernatants of infected LSECs, however, increased in all infected cells ($P \leq 0.001$) but remained higher in MHV3- and YAC-MHV3-infected cells than in 51.6-MHV3-infected cells ($P \leq 0.05$) (Fig. 8IF). The IL-6 mRNA expression reached higher levels in cells infected by virulent MHV3 than in those infected by attenuated strains only at 24 h p.i. ($P \leq 0.05$ to 0.001) (Fig. 8IG), correlating with higher release in supernatants of MHV3-infected cells ($P \leq 0.01$) (Fig. 8IH).

LSECs were also reported to secrete chemokines upon infection by dengue virus and to enhance their production in chronic inflammatory liver disease (39, 40). Thus, we presumed that MHV3-infected LSECs may produce higher levels of chemokines. As shown in Fig. 3IIA to D, CXCL1 and CCL2 expression was higher upregulated in MHV3-infected LSECs than in 51.6- and YAC-MHV3-infected cells at 24 and 48 h p.i., leading to larger amounts released in cell supernatants ($P \leq 0.05$ to 0.001). CXCL10 gene expression and production levels increased only in MHV3-infected LSECs ($P \leq 0.05$ to 0.001) (Fig. 8IIE and F).

Proinflammatory activation of LSECs by MHV3 depends on TLR2 signaling. We have previously shown that induction of in-

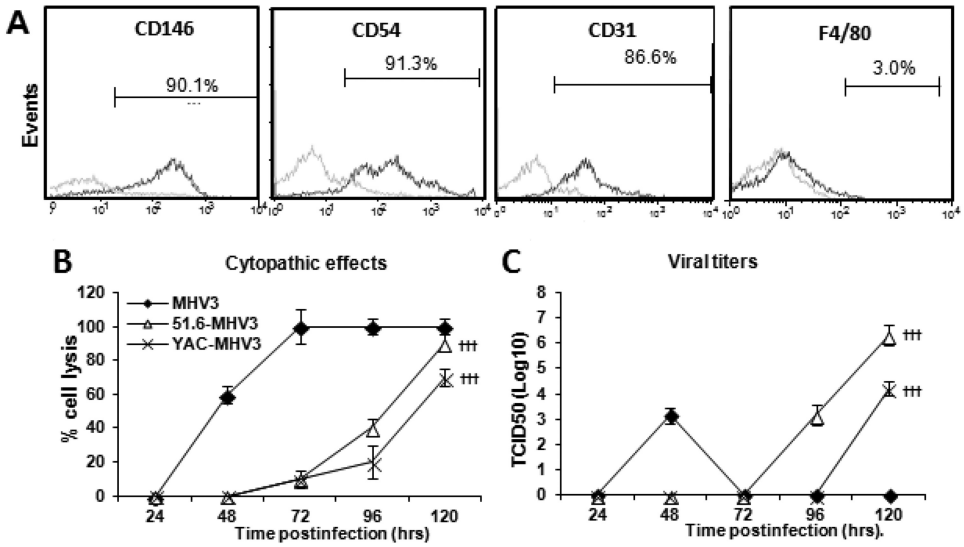

FIG 6 Permissivity of LSECs to MHV3, 51.6-MHV3, and YAC-MHV3 infection. Mouse LSECs were isolated with Percoll gradients and enriched by immunomagnetism with anti-CD146 antibodies. (A) LSECs were characterized by immunolabeling with antibodies for CD146, CD54, CD31, and F4/80 cell markers and cytofluorometric analysis. (B and C) LSECs were infected at an MOI of 0.1 with MHV3, 51.6-MHV3, and YAC-MHV3. The evolution of cytopathic effects in LSEC cultures was noted up to 5 days p.i. (B), and the kinetics of MHV infections were monitored by quantifying viral titers in supernatants of infected LSECs (C). All experiments were conducted in triplicate. Results are representative of two independent experiments. Values are means for each point. †††, $P < 0.001$ compared with MHV3-infected cells.

flammatory cytokines by MHV3 in *in vitro*-infected macrophages depended on TLR2 signaling (37). In addition, Liu et al. (9) recently demonstrated that TLR2 activation on LSECs reversed their anti-inflammatory functions. Since TLR2 was strongly upregulated in livers from MHV3-infected mice, we aimed to investigate whether TLR2 was involved in the conversion of LSECs toward a proinflammatory profile. We first sought to determine whether MHV3 increased TLR2 expression on LSECs. As shown in Fig. 9A, levels of TLR2 mRNAs were significantly higher in cells infected by MHV3 than in those infected by attenuated strains at 24 h p.i. ($P \leq$ 0.05 to 0.01). To address whether TLR2 was involved in the cytokine response and viral replication in infected LSECs, TLR2 expression was abrogated by siRNAs prior to infection, and IL-6 and CXCL1 mRNA levels were determined by qRT-PCR at 24 h p.i. Viral replication of MHV3, but that of not 51.6- and YAC-MHV3, was significantly reduced following TLR2 knockdown ($P \leq 0.001$) (Fig. 9B). A markedly decreased expression of IL-6 and CXCL1 levels and an upregulation of IL-10 levels were also observed in MHV3-infected cells rendered defective for TLR2, while no difference was noted in cells infected with the attenuated variants ($P \leq 0.001$) (Fig. 9C to E). These results suggest that the higher tropism and proinflammatory induction capacities of MHV3 in LSECs reflect its unique ability to activate TLR2 signaling.

TLR2 exacerbates liver damage and increases viral replication in mice infected by virulent but not attenuated MHV3 strains. We already reported that MHV3-induced acute hepatitis was less severe in TLR2 KO mice (41). To verify whether TLR2 is differentially involved in the evolution of hepatitis induced by virulent and attenuated MHV3 strains, groups of wild-type (WT) C57BL/6 and TLR2 knockout (KO) mice were i.p. infected with MHV3 or 51.6-MHV3. The survival rate was monitored, and liver damage and viral load were evaluated at 72 h p.i. As shown in Fig. 10A and B, survival of TLR2 KO mice infected by MHV3, but not 51.6-MHV3, was prolonged compared to that of the respective infected WT mice ($P \leq 0.001$). Accordingly, histopathological analysis of the liver revealed fewer and smaller necrotic foci in MHV3-infected TLR2 KO mice than in WT mice, whereas comparable and barely detectable hepatic damage was noted in TLR2 KO and WT mice infected with 51.6-MHV3 (Fig. 10C).

In addition, viral replication of MHV3 at 72 h p.i. was lower in the livers of infected TLR2 KO mice than in those of WT mice, whereas 51.6-MHV3 replication was similar in both mouse strains (Fig. 10D) ($P \leq 0.001$). Taken together, these results suggest that TLR2 aggravates hepatic damage and viral replication in mice infected by virulent but not attenuated MHV3 strains.

TLR2 activation by virulent MHV3 decreases IL-10 and increases inflammatory cytokine and chemokine expression. It was previously reported that hepatic levels of IL-6 and TNF-α were reduced in MHV3-infected TLR2 KO mice in comparison to C57BL/6 mice, suggesting a role for TLR2 in MHV3-induced release of inflammatory factors (41). Thus, we speculated that MHV3, in contrast to 51.6-MHV3, may promote a proinflammatory cytokine profile in the liver through TLR2 activation, such as observed in *in vitro*-infected LSECs. To test this hypothesis, expression levels of several inflammatory and anti-inflammatory factors were compared between livers from TLR2 KO and wild-type (WT) mice infected with both viruses. As shown in Table 2, lower TNF-α, IL-6, CXCL1, CCL2, and CXCL10 mRNA expression and higher IL-10 levels occurred in the livers of MHV3-infected TLR2 KO mice compared to those of WT mice ($P \leq 0.001$), whereas levels of Fgl2 and IL-33 were similar in both mouse strains. In contrast, no difference was observed between cytokine profile in 51.6-MHV3-infected WT and TLR2 KO mice, albeit a slight reduction of CXCL10 expression was noted in TLR2 KO mice ($P \leq 0.05$). Given the importance of IL-10 in the control of hepatic inflammation, we aimed to determine whether higher lev-

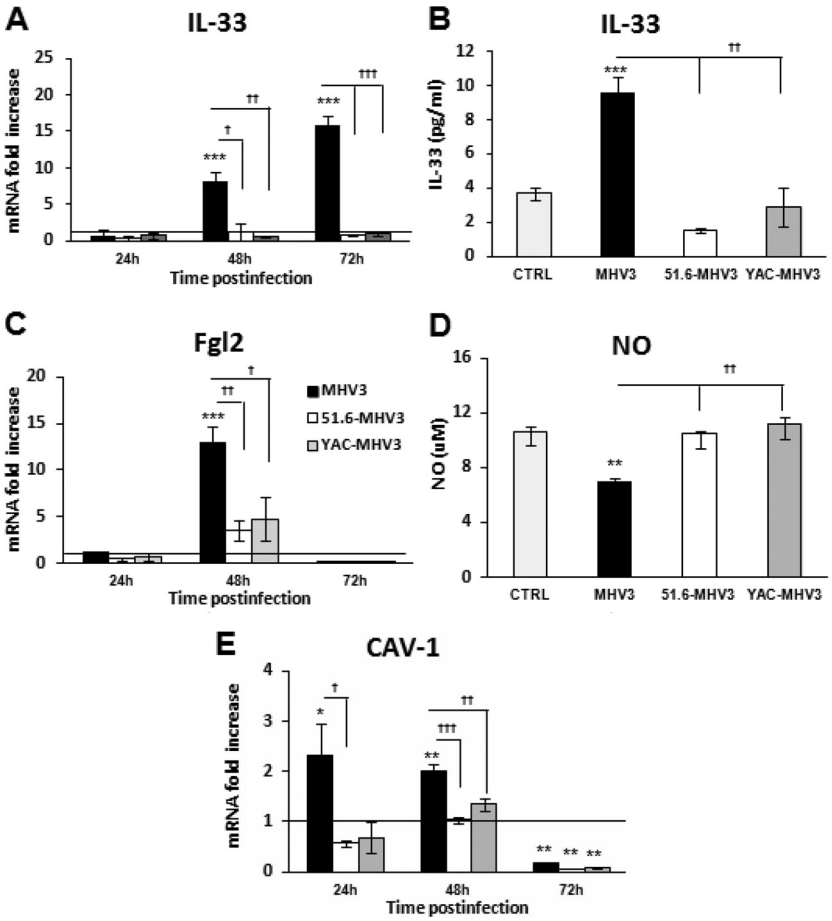

FIG 7 Expression levels of Fgl2, IL-33, and caveolin-1 and production of NO in *in vitro* MHV3-, 51.6-MHV3-, and YAC-MHV3-infected LSECs. LSECs were infected at an MOI of 0.1 with MHV3, 51.6-MHV3, and YAC-MHV3, and RNA and supernatant from LSECs infected with each viral strain were collected at 24, 48, or 72 h p.i. (A, C, and E) IL-33 (A), Fgl2 (C), and caveolin-1 (E) mRNA fold changes were analyzed by qRT-PCR. Values represent fold change in gene expression relative to that in uninfected LSECs (control arbitrarily taken as 1) after normalization to HPRT expression. All samples were run in duplicate. (B and D) Production levels of IL-33 were quantified by ELISA (B) and NO levels were assayed by the Griess reaction (D) in supernatants at 48 h p.i. All experiments were run in duplicate, and results are representative of two independent experiments. Values are means and standard errors of the means. *, $P < 0.05$; **, $P < 0.01$; ***, $P < 0.001$ (compared with mock-infected cells). †, $P < 0.05$; ††, $P < 0.01$; †††, $P < 0.001$ (compared with MHV3-infected cells).

els in livers from MHV3-infected TLR2 KO mice reflected higher production by ECs. A double immunohistochemistry staining of IL-10 and CAV-1 on liver sections revealed that expression of IL-10 in ECs was effectively higher in livers from MHV3-infected TLR2 KO mice than in those from WT mice (Fig. 11; compare Fig. 3II).

DISCUSSION

In this work, we investigated the role of LSECs in hepatic inflammation during the acute viral hepatitis process using the MHV3 model of infection. We demonstrated that the severity of hepatitis, viral replication, and hepatic inflammation correlated with permissivity of LSECs for MHV3 strains and subsequent structural and functional disturbances. We showed that *in vitro* infection of LSECs by the virulent MHV3, in contrast to the attenuated 51.6- and YAC-MHV3 variants, resulted in earlier cell damage and disorders in inflammatory and vascular factors, as reflected by a high release of inflammatory cytokines/chemokines and procoagulant Fgl2 and a decrease in NO and IL-10 levels. We showed that the higher replication rate and proinflammatory activity of MHV3 in LSECs was associated with its specific activation of TLR2 signaling in LSECs and that TLR2 is a key factor of hepatic inflammation and LSEC-derived IL-10 disorders in MHV3-induced fulminant hepatitis.

LSECs, lining the hepatic sinusoids, mediate liver tolerance under physiological conditions (reviewed in reference 1), but these cells are the target of many hepatotropic viruses. The consequence of LSEC infection in inflammatory liver diseases such as viral hepatitis has never been investigated. We have shown that MHV3 infection induced differential structural and functional disorders in LSECs according to strain virulence. Indeed, the highly virulent MHV3 replicated faster and to higher levels in LSECs, leading to occurrence of CPE such as a change in morphology (rounded cells) and cell lysis from 48 h p.i. Previous reports have already shown that *in vivo* and *in vitro* infections of LSECs by MHV3 are associated with cell damage and loss of fenestrations (27), but no syncytial cells were observed. However, MHV3 did not replicate in LSECs as fast as it usually does

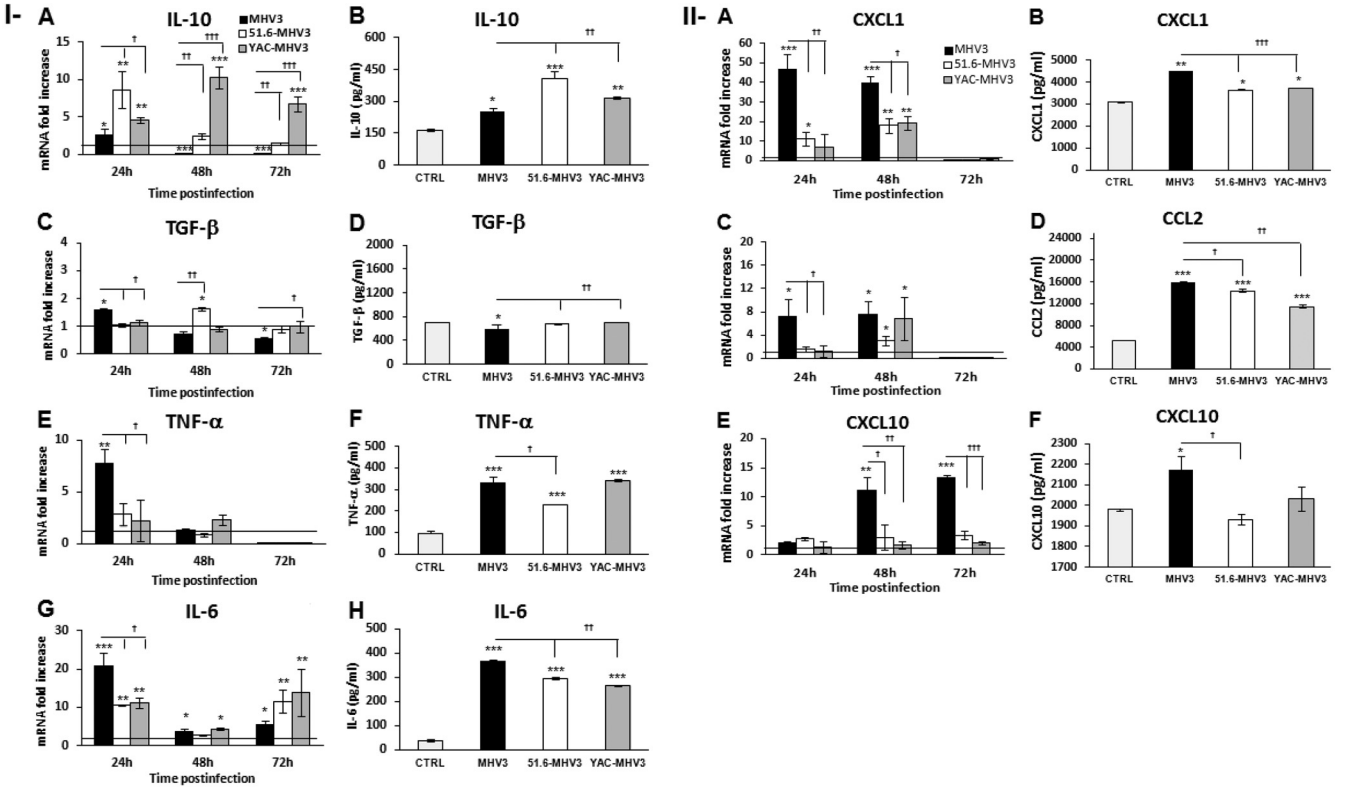

FIG 8 Gene expression and production of IL-10, TGF-β, IL-6, TNF-α, CXCL1, CCL2, and CXCL10 in *in vitro* MHV3-, 51.6-MHV3-, and YAC-MHV3-infected LSECs. LSECs were infected at an MOI of 0.1 with MHV3, 51.6-MHV3, and YAC-MHV3, and RNA and supernatant from LSECs infected with each viral strain were collected at 24, 48, or 72 h p.i. (I) Fold changes in IL-10 (A), TGF-β (C), IL-6 (E), and TNF-α (G) mRNA were analyzed by qRT-PCR. Values represent fold change in gene expression relative to that in uninfected LSECs (control arbitrarily taken as 1) after normalization to HPRT expression. All samples were run in duplicate. Production levels of IL-10 (B), TGF-β (D), IL-6 (F), and TNF-α (H) in supernatants were quantified by ELISA at 24 h p.i. (II) Fold changes in CXCL1 (A), CCL2 (C), and CXCL10 (E) mRNA were analyzed by qRT-PCR. Values represent fold change in gene expression relative to that in control (uninfected) LSECs after normalization to HPRT expression. All samples were run in duplicate. Production levels of CXCL1 (B), CCL2 (D), and CXCL10 (F) in supernatants were quantified by ELISA at 24 h p.i. All experiments were conducted in duplicate, and results are representative of two independent experiments. Values are means and standard errors of the means. *, $P < 0.05$; **, $P < 0.01$; ***, $P < 0.001$ (compared with mock-infected cells). †, $P < 0.05$; ††, $P < 0.01$; †††, $P < 0.001$ (compared with MHV3-infected cells).

in *in vitro*-cultured cells, since no viral burden was detected until 48 h p.i. while MHV3 titers are detectable within 24 h p.i. in macrophages (24, 41). Our results are nevertheless in accordance with those of Pereira et al. (26), who have shown that MHV3 replicates more rapidly in Kupffer cells (KCs) than in LSECs *in vitro*, suggesting that LSECs may transiently control the viral replication.

In agreement, replication of the attenuated 51.6- and YAC-MHV3 variants was delayed to 96 or 120 h p.i. and was associated with barely detectable CPE, reflecting their weaker tropism for LSECs. It was recently reported that LSECs exhibit a high capacity for clearance of circulating viruses (42, 43), suggesting that they may have a high ability to sequester attenuated but not virulent MHV3 particles. However, the fact that replication of MHV3 variants in LSECs was delayed but not aborted suggests, rather, a host cell-dependent mechanism of control of viral replication. Indeed, preliminary results showed a higher antiviral IFN-β response in LSECs infected by attenuated MHV3 strains (results not shown). The low IFN-β response in virulent MHV3-infected LSECs may be related to specific viral evasion mechanisms from host viral sensors or interference with downstream signaling pathways. We have observed that MHV3, in contrast to attenuated strains, induced neither TLR3 nor RIG-I expression in LSECs (results not shown), suggesting lower detection by these viral sensors. Further work should address whether viral products or evasion strategies are involved in MHV3-induced impairment of the IFN-β response in LSECs.

The inability of attenuated MHV3 variants to establish a rapid infection in LSECs correlated with a less severe hepatitis. Indeed, 51.6-MHV3 infection resulted in lower viral replication, transaminase levels, and liver damage than MHV3 infection. The 51.6-MHV3 variant differs from the pathogenic MHV3 only by its weaker tropism for LSECs but retains its virulence for hepatocytes, KCs, and Ito cells (24), suggesting that resistance of LSECs to viral replication may protect against fulminant hepatitis. Similarly, the nonpathogenic YAC-MHV3, also with a low ability to replicate in LSECs, induced light and transient hepatic lesions, reinforcing the importance of functional integrity of LSECs in the evolution of viral hepatitis. Indeed, less severe hepatic damage and viral load in mice infected with the attenuated variants may possibly result from a better early control of viral replication by LSECs, leading to reduced transmission of viral progeny to the hepatic parenchyma. In agreement, a delayed replication of MHV3 in LSECs was suggested as a crucial step in the resistance of various strains of mice

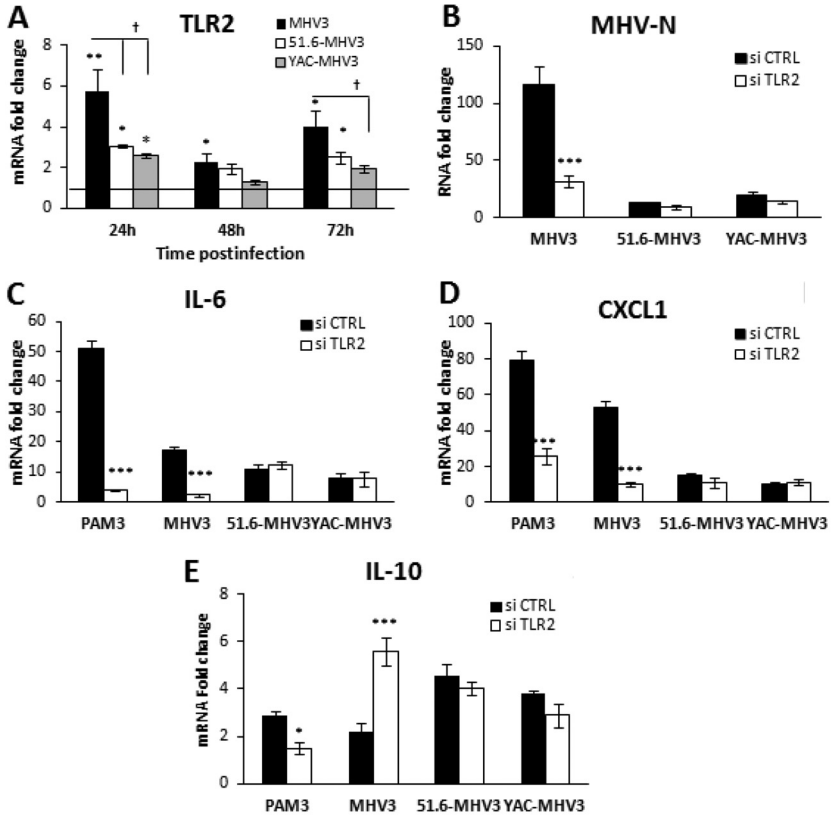

FIG 9 Role of TLR2 in viral replication and expression of IL-6 and CXCL1 in MHV3-, 51.6-MHV3-, and YAC-MHV3-infected LSECs. (A) LSECs were infected at an MOI of 0.1 with MHV3, 51.6-MHV3, and YAC-MHV3. At 24, 48, and 72 h p.i., RNA from infected LSECs was extracted and mRNA expression levels for the TLR2 gene were determined by qRT-PCR. (B to D) LSECs were treated with a specific siRNA against TLR2 prior to infection with viruses or treatment with the specific TLR2 agonist Pam3Cys (as a positive control) for 24 h. mRNA expression levels of MHV nucleoprotein (MHV-N) (B), IL-6 (C), and CXCL1 (D) were determined by qRT-PCR. Values represent fold change in gene expression relative to that in control (uninfected) LSECs after normalization to HPRT expression. All samples were run in duplicate, and results are representative of two independent experiments. *, $P < 0.05$; **, $P < 0.01$; ***, $P < 0.001$ (compared with control cells). †, $P < 0.05$ (compared with MHV3-infected cells).

to MHV3 infection by allowing time for the local and systemic responses to clear the infective particles (26).

We report here for the first time that *in vitro* MHV3 infection promotes a proinflammatory activation of LSECs. Indeed, MHV3 induced higher levels of IL-6, TNF-α, and chemokines in LSECs than attenuated strains and inhibited their basal release of IL-10, while attenuated strains enhanced it. These inflammatory disorders in LSECs correlated with higher ratios of intrahepatic inflammatory to anti-inflammatory mediators in the livers of MHV3-infected mice, suggesting that LSECs may have lost their ability to control inflammation. In agreement, IL-10 staining was significantly lower in ECs from the livers of mice infected by MHV3 than in those of mice infected by attenuated strains. The importance of IL-10 production by LSECs in the suppression of proinflammatory cytokine release by Th1 and Th17 cells was recently shown by Carambia et al. (44). In addition, LSECs were recently shown to be more efficient than KCs in tolerizing autoreactive Th1 cells via IL-10 (2). The lower inflammatory profiles in livers from 51.6- and YAC-MHV3-infected mice are in line with our previous observations (30). The highly attenuated YAC-MHV3 infection correlated with lower induction of inflammatory mediators than 51.6-MHV3 infection. Higher levels of anti-inflammatory IL-10 and immunosuppressive PGE_2 in the livers of YAC-MHV3- than in those of 51.6-MHV3-infected mice were reported previously (30), suggesting that the highly attenuated phenotype of YAC-MHV3 may reflect the preservation of integrity of LSECs and other, yet-unidentified hepatic cells. Since YAC-MHV3, unlike 51.6-MHV3, was shown to replicate less in macrophages *in vitro* (45), it is plausible that preservation of KC tolerance functions may further contribute to lower inflammatory responses during YAC-MHV3 infection. Altogether, the results from YAC-MHV3 and 51.6-MHV3 infections strengthen the importance of LSEC structural and functional integrity in restricting the hepatic inflammatory response and subsequent damage. In agreement, activation of LSECs toward a proinflammatory profile was pointed out as a critical component of intrahepatic inflammation in hepatic fibrosis (40).

Differences in the LSEC cytokine profile according to infection by pathogenic or attenuated MHV3 strains may reflect differential PRR induction and activation by viral fixation and/or replication. We have already demonstrated that IL-6 and TNF-α production by MHV3-infected macrophages resulted from TLR2 activation by the surface (S) viral protein (41). The production of TNF-α by LSECs is known to depend on TLR1 to -4, -6, and -8, while IL-6 is produced following activation of TLR1 to -4 only (4, 17). It has been recently demonstrated that TLR1/2 ligand (PamC3), but not

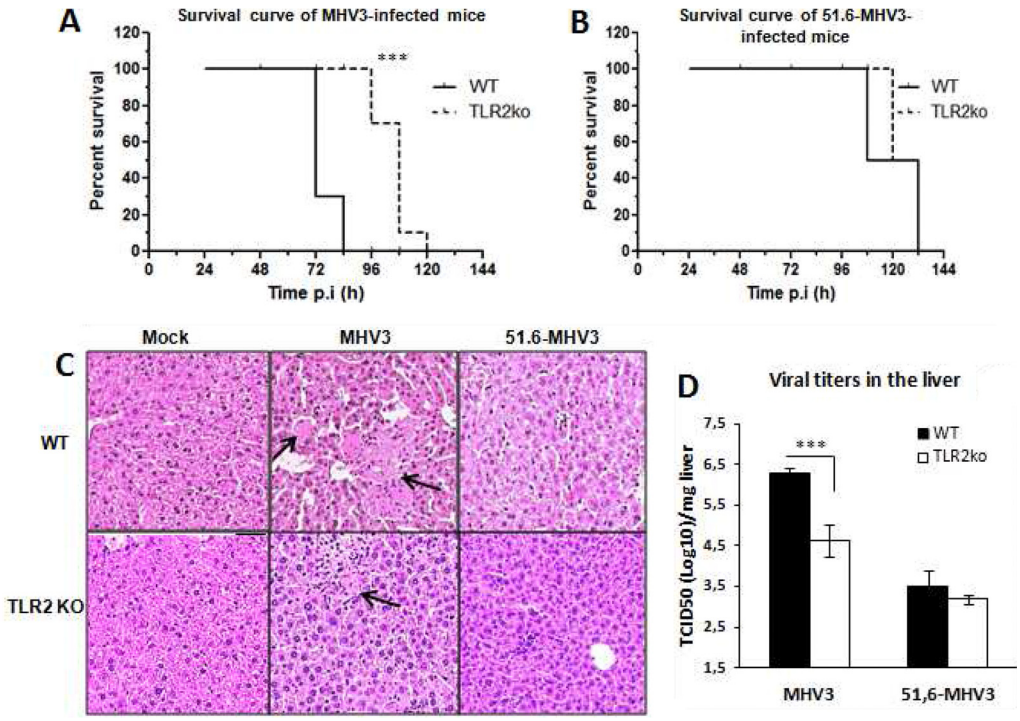

FIG 10 Mortality, hepatic damage, and viral replication in MHV3- and 51.6-MHV3-infected C57BL/6 (WT) and TLR2 KO mice. Groups of 6 or 7 C57BL/6 (WT) and TLR2 KO mice were intraperitoneally (i.p.) infected with 1,000 $TCID_{50}$ of MHV3 and 51.6-MHV3. (A and B) Percentages of MHV3-infected (A) and 51.6-MHV3-infected (B) surviving mice were recorded at various times postinfection (p.i.). (C) Histopathological analysis was conducted on livers from mock-, MHV3-, and 51.6-MHV3-infected WT and TLR2 KO mice at 72 h p.i. Necrotic foci are indicated by arrows. (D) MHV3 and 51.6-MHV3 replication in livers from infected WT and TLR2 KO mice was determined by viral titration ($TCID_{50}$) at 24 h and 72 h p.i. Values are means and standard errors of the means. Results are representative of two different experiments. ***, $P < 0.001$ compared with WT mice.

TLR3 ligand [poly(I·C)] or LPS, reverted the suppressive properties of LSECs (9). We have shown that the virulent MHV3 strain highly induced TLR2 expression on cultured LSECs and that TLR2 knockdown abrogated IL-6 and CXCL1 induction only in LSECs infected by MHV3. Indeed, the proinflammatory activity of MHV3 may be related to its unique ability to induce TLR2 signaling. In agreement, lower levels of inflammatory cytokines and chemokines were observed in the livers of MHV3-infected TLR2 KO mice, correlating with milder hepatic damage and delayed mortality of mice. Thus, TLR2 activation may represent one determining and differential factor involved in the severity of virulent versus attenuated MHV3-induced hepatitis. In line with this hypothesis, the survival rate, inflammatory response, and liver damage were similar in TLR2 KO and WT mice infected by 51.6-MHV3 and were comparable to those observed in MHV3-infected TLR2 KO mice. Furthermore, IL-10 levels were significantly higher in MHV3-infected TLR2 KO mice, with increased expression on ECs and also on some CAV-1 negative cells, suggesting that specific activation of TLR2 by the virus could be one mechanism by which MHV3 reverts the anti-inflammatory phenotype, at least in LSECs. Supporting this assumption, IL-10 expression was significantly upregulated in *in vitro*-MHV3-infected LSECs treated with siTLR2, suggesting an inhibitory effect for TLR2 on IL-10 induction by MHV3. Accordingly, TLR2 activation has already been shown to temporarily reverse Treg suppressive functions (46, 47). Further work will be done to identify other IL-10-producing CAV-1-negative cells during MHV3 infection.

TLR2 may also potentiate MHV3 infection, as viral replication was significantly reduced in the livers of TLR2 KO mice and in cultured LSECs rendered defective for TLR2. In addition, activation of TLR2 by MHV3 may account for its higher replication rate

TABLE 2 Transcription levels of several genes in livers from MHV3- and 51.6-MHV3-infected C57BL/6 (WT) and TLR2 KO mice at 72 h p.i.[a]

	Fold change (mean ± SEM)[b]			
	MHV3 infection		51.6-MHV3 infection	
Gene	WT	TLR2 KO	WT	TLR2 KO
TNF-α	70.2 ± 7.2	44.9 ± 4.0***	10.5 ± 1.03	7.1 ± 2.8
IL-6	43.5 ± 5.7	11.2 ± 5.0***	13 ± 1.4	14 ± 7.4
IL-10	5.8 ± 1.4	44 ± 11.7***	54.5 ± 17.4	41.4 ± 3.8
CXCL1	131 ± 15	21.1 ± 8.7***	107 ± 4.9	91 ± 11.9
CCL2	1,027 ± 134	155 ± 37***	147 ± 14.8	120.4 ± 39.1
CXCL10	213 ± 20	69 ± 15***	33.7 ± 7.4	17.5 ± 4.8*
Fgl2	6.65 ± 0.70	10.1 ± 1.2	6.7 ± 0.7	4.7 ± 1.7
IL-33	4.5 ± 0.4	3.7 ± 0.3	ND	ND

[a] Groups of 5 or 6 C57BL/6 (WT) or TLR2 KO mice were intraperitoneally infected with 1,000 $TCID_{50}$ of MHV3 or 51.6-MHV3. At 72 h p.i., livers were collected from mock- and virus-infected mice from each group, and mRNA fold changes for several genes were analyzed by qRT-PCR.

[b] Values represent fold change in gene expression relative to that in mock-infected mice after normalization to HPRT expression. Samples from each mouse were run in duplicate. Values that are significantly different between MHV3-infected TLR2 KO and C57BL/6 (WT) mice or between 51.6-MHV3-infected TLR2 KO and C57BL/6 (WT) mice are indicated by asterisks as follows: ***, $P < 0.01$; *, $P < 0.5$. ND not detectable.

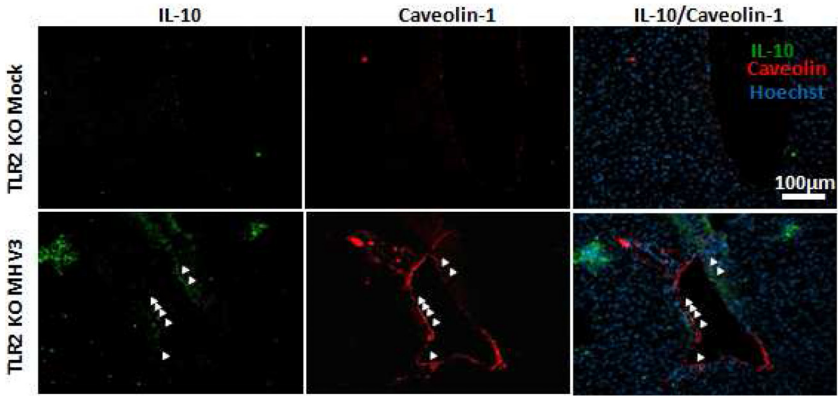

FIG 11 Expression of IL-10 and caveolin-1 in livers from MHV3-infected TLR2 KO mice. Groups of 6 TLR2 KO mice were intraperitoneally (i.p.) infected with 1,000 $TCID_{50}$ of MHV3, and immunolocalization of IL-10 in the livers and ECs of mock- and MHV3-infected TLR2 KO mice was determined by double immunostaining of IL-10 (green) and caveolin-1 (red) at 48 h p.i. Cell nuclei were counterstained with Hoechst stain (blue). *In situ* expression of IL-10 and caveolin-1 by endothelial cells is indicated by arrows.

in LSECs, since the replication of 51.6-MHV3 was not influenced by TLR2 in infected LSECs or mice. It has been demonstrated that MHV replication depends on the activation of the P38 mitogen-activated protein kinase (MAPK) at the beginning of the replicative cycle (48). Thus, it is conceivable that activation of TLR2 by MHV3 on LSECs optimizes P38 MAPK activation, predisposing to more efficient viral replication. Since TLR2 is also expressed, though to a lesser extent, by other resident or recruited cells in the liver, such as KCs, neutrophils, and hepatocytes, as observed in preliminary experiments, we can hypothesize that several $TLR2^+$ cell types permissive to MHV3 infection may act synergistically in promoting viral replication and hepatic inflammation. Indeed, preliminary *in vitro* results revealed that production of inflammatory mediators and viral replication in MHV3-infected hepatocytes and macrophages were enhanced by TLR2. Further work is in progress to clarify the mechanistic implications of TLR2 in MHV3 replication and the role of recruited and resident $TLR2^+$ inflammatory cells in hepatic inflammation and damage.

The differences in chemokine levels induced by the pathogenic and attenuated MHV3 strains may explain the differences in recruited intrahepatic leukocyte subsets. Indeed, lower levels of CXCL1 and CCL2 in livers from 51.6- and YAC-MHV3-infected mice correlated with delayed or lower intrahepatic recruitment of neutrophils and macrophages, thus explaining the smaller inflammatory foci without extensive necrosis areas seen in livers from these mice. Unexpectedly, neutrophils were only transiently recruited, and the numbers of NK-T, T, and B lymphocytes progressively decreased throughout MHV3 infection, despite high induction of chemokines. We have previously demonstrated that intrahepatic NK and NK-T cells undergo higher apoptosis and that B and T cells are more strongly depleted in lymphoid organs during MHV3 infection than during YAC-MHV3 infection (30, 31, 49), thus altering lymphocyte recruitment or turnover into the liver. The highly attenuated YAC-MHV3 infection, compared to MHV3, was also related to effective activation of $CD8^+$ cells (32).

In addition, impairment of intrahepatic leukocyte populations and severe liver injury in MHV3-infected mice may also be connected to disturbances in LSEC-derived vascular factors. We have demonstrated that MHV3, unlike attenuated variants, significantly altered NO release by LSECs. Susceptibility of mice to MHV3 infection has already been inversely correlated with NO levels in the liver, but the mechanism was not elucidated (50). The constitutive expression of NO by LSECs is essential for the regulation of intrahepatic sinusoidal blood flow and protects against liver diseases. Indeed, impairment of NO release by LSECs has been associated with hepatic microvascular dysfunction and portal hypertension in pathological liver conditions such as fibrosis and cirrhosis (37). In cirrhotic livers, an NO defect has been linked to overexpression of CAV-1, a negative regulator of the endothelial NO synthase activity, on LSECs (38). We have observed that reduced NO levels in LSECs correlated with a concomitant upregulation of CAV-1, supporting that MHV3-induced NO impairment is indirectly related to CAV-1 induction. Furthermore, we have demonstrated that expression of the procoagulant Fgl2 increased only in LSECs infected by MHV3. MHV3-induced expression of Fgl2 has already been reported in endothelium of intrahepatic veins and sinusoids and was associated with severe intravascular coagulation, ischemia, and liver necrosis in MHV3-infected mice (28). In agreement, liver histopathological analysis revealed vascular thrombosis and fibrin deposition in hepatic veins and sinusoids from 48 h p.i. in MHV3-infected mice only (results not shown). No difference in Fgl2 levels was observed between MHV3-infected WT and TLR2 KO mice, indicating that induction of Fgl2 in LSECs is TLR2 independent. Since Fgl2 expression in LSECs was reported to be promoted by the MHV nucleocapsid protein and TNF-α (51, 52), we can assume that higher induction of Fgl2 in the livers of MHV3-infected mice may reflect higher hepatic TNF-α levels and viral replication rate in LSECs. Thus, the combined effect of CAV-1/NO imbalance and Fgl2 induction during MHV3 infection may contribute to alter leukocyte recruitment and aggravate hepatitis in disturbing hepatic microcirculation.

The alarmin IL-33 was shown to be upregulated in LSECs during chronic HBV and HCV infections and acute liver failure, but the mechanism is elusive (21, 22). In agreement with our previous report, MHV3 infection increased IL-33 production in both LSECs and hepatocytes (29). Our results showed that IL-33 expression in LSECs was increased only by virulent

MHV3 and was not modulated by TLR2, suggesting that IL-33 release is rather a consequence of MHV3-induced cell damage, as necrotic cells in the liver were shown to secrete alarmins such as HMGB-1 and IL-33 (53). In addition, a high IL-33 serum level was associated with liver damage in HBV and HCV infections, indicating that IL-33 could be considered a predictive indicator of viral hepatitis evolution, as previously suggested (54, 55).

Using the MHV3 animal model of viral acute hepatitis, this work suggests a novel virus-promoted mechanism of hepatic inflammation and damage involving disorders in LSEC-derived inflammatory and vascular factors. The use of MHV3 variants expressing weak tropism for LSECs allowed us to better discriminate the importance of LSECs, over that of other hepatic cells, in tolerance/inflammation imbalance during acute viral infection. Our results support that induction of TLR2-dependent reversion of LSEC anti-inflammatory functions by MHV3 may participate in the pathological inflammatory response that predisposes to fulminant hepatitis. Unlike MHV3, HCV and HBV do not productively infect LSECs, but RNA from HCV was recently shown to induce the expression of inflammatory cytokines and chemokines in human microvascular endothelial cells via TLR3 activation (56), indicating that LSECs can be activated through PRR engagement by HCV-derived products. The "core" protein of HCV and HBV was reported to bind to TLR2 and induce a TLR2-dependent inflammatory cytokine response in monocytes and macrophages (57, 58). Thus, one could presume that core proteins could also promote proinflammatory activation of LSECs via TLR2, aggravating hepatic inflammation. In this regard, a high correlation between TLR2 expression and hepatic inflammation and necrosis was demonstrated in the livers of HCV-infected patients (59).

ACKNOWLEDGMENTS

We acknowledge Corentine Lux, Pascale Bellaud, and Eric Massicotte for their technical assistance.

FUNDING INFORMATION

This work was funded by the government of Canada through NSERC grant 2895-2009 to Lucie Lamontagne. Christian Bleau was supported by an NSERC fellowship. The funders had no role in study design, data collection and interpretation, or the decision to submit the work for publication.

REFERENCES

1. **Tiegs G, Lohse AW.** 2010. Immune tolerance: what is unique about the liver. J Autoimmun **34:**1–6. http://dx.doi.org/10.1016/j.jaut.2009.08.008.
2. **Xu X, Jin R, Li M, Wang K, Zhang S, Hao J, Sun X, Zhang Y, Wu H, Zhang J, Ge Q.** 2016. Liver sinusoidal endothelial cells induce tolerance of autoreactive CD4(+) recent thymic emigrants. Sci Rep **6:**19861. http://dx.doi.org/10.1038/srep19861.
3. **Thomson AW, Knolle PA.** 2010. Antigen-presenting cell function in the tolerogenic liver environment. Nat Rev Immunol **10:**753–766. http://dx.doi.org/10.1038/nri2858.
4. **Oda M, Yokomori H, Han JY.** 2003. Regulatory mechanisms of hepatic microcirculation. Clin Hemorheol Microcirc **29:**167–182.
5. **Kern M, Popov A, Scholz K, Schumak B, Djandji D, Limmer A, Eggle D, Sacher T, Zawatzky R, Holtappels R, Reddehase MJ, Hartmann G, Debey-Pascher S, Diehl L, Kalinke U, Koszinowski U, Schultze J, Knolle PA.** 2010. Virally infected mouse liver endothelial cells trigger CD8+ T-cell immunity. Gastroenterology **138:**336–346. http://dx.doi.org/10.1053/j.gastro.2009.08.057.
6. **Wu J, Meng Z, Jiang M, Zhang E, Trippler M, Broering R, Bucchi A, Krux F, Dittmer U, Yang D, Roggendorf M, Gerken G, Lu M, Schlaak JF.** 2010. Toll-like receptor-induced innate immune responses in non-parenchymal liver cells are cell type-specific. Immunology **129:**363–374. http://dx.doi.org/10.1111/j.1365-2567.2009.03179.x.
7. **Bissell DM, Wang SS, Jarnagin WR, Roll FJ.** 1995. Cell-specific expression of transforming growth factor-beta in rat liver. Evidence for autocrine regulation of hepatocyte proliferation. J Clin Invest **96:**447–455.
8. **Knolle PA, Uhrig A, Hegenbarth Löser S E, Schmitt E, Gerken G, Lohse AW.** 1998. IL-10 down-regulates T cell activation by antigen-presenting liver sinusoidal endothelial cells through decreased antigen uptake via the mannose receptor and lowered surface expression of accessory molecules. Clin Exp Immunol **114:**427–433. http://dx.doi.org/10.1046/j.1365-2249.1998.00713.x.
9. **Liu J, Jiang M, Ma Z, Dietze KK, Zelinskyy G, Yang D, Dittmer U, Schlaak JF, R oggendorf, Lu MM.** 2013. TLR1/2 ligand-stimulated mouse liver endothelial cells secrete IL-12 and trigger CD8+ T cell immunity in vitro. J Immunol **191:**6178–6190. http://dx.doi.org/10.4049/jimmunol.1301262.
10. **Lavanchy D.** 2009. The global burden of hepatitis C. Liver Int **29:**74–81. http://dx.doi.org/10.1111/j.1478-3231.2008.01934.x.
11. **Yang Q, Shi Y, Yang Y, Lou G, Chen Z.** 2015. The sterile inflammation in the exacerbation of HBV-associated liver injury. Mediators Inflamm **2015:**508681. http://dx.doi.org/10.1155/2015/508681.
12. **Bortolami M, Kotsafti A, Cardin R, Farinati F.** 2008. Fas/FasL system, IL-1beta expression and apoptosis in chronic HBV and HCV liver disease. J Viral Hepat **15:**515–522. http://dx.doi.org/10.1111/j.1365-2893.2008.00974.x.
13. **Barnaba V.** 2010. Hepatitis C virus infection: a "liaison a trois" amongst the virus, the host, and chronic low-level inflammation for human survival. J Hepatol **53:**752–761. http://dx.doi.org/10.1016/j.jhep.2010.06.003.
14. **Liu M, Chan WY, McGilvray I, Ning Q, Levy GA.** 2001. Fulminant viral hepatitis: molecular and cellular basis, and clinical implications. Exp Rev Mol Med **3:**1–19. http://dx.doi.org/10.1017/S1462399401002575.
15. **Breiner KM, Schaller H, Knolle PA.** 2001. Endothelial cell-mediated uptake of a hepatitis B virus: a new concept of liver targeting of hepatotropic microorganisms. Hepatology **34:**803–808. http://dx.doi.org/10.1053/jhep.2001.27810.
16. **Pöhlmann S, Zhang J, Baribaud F, Chen K, Leslie GJ, Lin G, Granelli Piperno A, Doms RW, Rice CM, McKeating JA.** 2003. Hepatitis C virus glycoproteins interact with DC-SIGN and DC-SIGNR. J Virol **77:**4070–4080. http://dx.doi.org/10.1128/JVI.77.7.4070-4080.2003.
17. **Broering R, Wu J, Meng Z, Hilgard P, Lu M, Trippler M, Szczeponek A, Gerken G, Schlaak JF.** 2008. Toll-like receptor-stimulated non-parenchymal liver cells can regulate hepatitis C virus replication. J Hepatol **48:**914–922. http://dx.doi.org/10.1016/j.jhep.2008.01.028.
18. **Ludwig IS, Lekkerkerker AN, Depla E, Bosman F, Musters RJ, Depraetere S, van Kooyk Y, Geijtenbeek TB.** 2004. Hepatitis C virus targets DC SIGN and LSIGN to escape lysosomal degradation. J Virol **78:**8322–8332. http://dx.doi.org/10.1128/JVI.78.15.8322-8332.2004.
19. **Zhu CL, Yan WM, Zhu F, Zhu YF, Xi D, Tian DY, Levy G, Luo XP, Ning Q.** 2005. Fibrinogen-like protein 2 fibroleukin expression and its correlation with disease progression in murine hepatitis virus type 3-induced fulminant hepatitis and in patients with severe viral hepatitis B. World J Gastroenterol **11:**6936–6940. http://dx.doi.org/10.3748/wjg.v11.i44.6936.
20. **Foerster K, Helmy A, Zhu Y, Khattar R, Adeyi OA, Wong KM, Shalev I, Clark DA, Wong PY, Heathcote EJ, Phillips MJ, Grant DR, Renner EL, Levy GA, Selzner N.** 2010. The novel immunoregulatory molecule FGL2a potential biomarker for severity chronic hepatitis C virus infection. J Hepatol **53:**608–615. http://dx.doi.org/10.1016/j.jhep.2010.04.020.
21. **Marvie P, Lisbonne M, L'Helgoualc'h A, Rauch M, Turlin B, Preisser L, Bourd-Boittin K, Théret N, Gascan H, Piquet-Pellorce C, Samson M.** 2010. Interleukin-33 overexpression is associated with liver fibrosis in mice and humans. J Cell Mol Med **14:**1726–1739. http://dx.doi.org/10.1111/j.1582-4934.2009.00801.x.
22. **Roth GA, Zimmermann M, Lubsczyk BA, Pilz J, Faybik P, Hetz H, Hacker S, Mangold A, Bacher A, Krenn CG, Ankersmit HJ.** 2010. Up-regulation of interleukin 33 and soluble ST2 serum levels in liver failure. J Surg Res **163:**e79–e83. http://dx.doi.org/10.1016/j.jss.2010.04.004.
23. **Le Prevost C, Virelizier JL, Dupuy JM.** 1975. Immunopathology of mouse hepatitis virus type 3 infection. III. Clinical and virologic observation of a persistent viral infection. J Immunol **115:**640–645.

24. **Martin JP, Chen Koehren WF, Pereira CA.** 1994. The virulence of mouse hepatitis virus 3, as evidenced by permissivity of cultured hepatic cells toward escaped mutants. Res Virol **145:**297–302. http://dx.doi.org/10.1016/S0923-2516(07)80034-3.
25. **Belouzard S, Millet JK, Licitra BN, Whittaker GR.** 2012. Mechanisms of coronavirus cell entry mediated by the viral spike protein. Viruses **4:**1011–1033. http://dx.doi.org/10.3390/v4061011.
26. **Pereira CA, Steffan AM, Kirn A.** 1984. Interaction between mouse hepatitis viruses and primary cultures of Kupffer and endothelial liver cells from resistant and susceptible inbred mouse strains. J Gen Virol **65:**1617–1620. http://dx.doi.org/10.1099/0022-1317-65-9-1617.
27. **Steffan AM, Pereira CA, Bingen A, Valle M, Martin JP, Koehren F, Royer C, Gendrault JL, Kirn A.** 1995. Mouse hepatitis virus type 3 infection provokes a decrease in the number of sinusoidal endothelial cell fenestrae both in vivo and in vitro. Hepatology **22:**395–401.
28. **Marsden PA, Ning Q, Fung S, Luo X, Chen Y, Mendicino M, Ghanekar A, Scott JA, Miller T, Chan CW, Chan MW, He W, Gorczynski RM, Grant DR, Clark DA, Phillips MJ, Levy GA.** 2003. The Fgl2/fibroleukin prothrombinase contributes to immunologically mediated thrombosis in experimental and human viral hepatitis. J Clin Invest **112:**58–6626. http://dx.doi.org/10.1172/JCI18114.
29. **Arshad MI, Patrat-Delon S, Piquet-Pellorce C, L'helgoualc'h A, Rauch M, Genet V, Lucas-Clerc C, Bleau C, Lamontagne L, Samson M.** 2013. Pathogenic mouse hepatitis virus or poly(I:C) induce IL-33 in hepatocytes in murine models of hepatitis. PLoS One **8:**e74278. http://dx.doi.org/10.1371/journal.pone.0074278.
30. **Jacques A, Bleau C, Martin JP, Lamontagne L.** 2008. Intrahepatic endothelial and Kupffer cells involved in immunosuppressive cytokines and natural killer (NK)/NK T cell disorders in viral acute hepatitis. Clin Exp Immunol **152:**298–310. http://dx.doi.org/10.1111/j.1365-2249.2008.03628.x.
31. **Lehoux M, Jacques A, Lusignan S, Lamontagne L.** 2004. Murine viral hepatitis involves NK cell depletion associated with virus-induced apoptosis. Clin Exp Immunol **137:**41–51. http://dx.doi.org/10.1111/j.1365-2249.2004.02501.x.
32. **Lamontagne L, Lusignan S, Page C.** 2001. Recovery from mouse hepatitis virus infection depends on recruitment of CD8(+) cells rather than activation of intrahepatic CD4(+)alphabeta(−)TCR(inter) or NK-T cells. Clin Immunol **101:**345–356. http://dx.doi.org/10.1006/clim.2001.5131.
33. **Schrage A, Loddenkemper C, Erben U, Lauer U, Hausdorf G, Jungblut PR, Johnson J, Knolle PA, Zeitz M, Hamann A, Klugewitz K.** 2008. Murine CD146 is widely expressed on endothelial cells and is recognized by the monoclonal antibody ME-9F1. Histochem Cell Biol **129:**441–451. http://dx.doi.org/10.1007/s00418-008-0379-x.
34. **Yamazaki H, Oda M, Takahashi Y, Iguchi H, Yoshimura K, Okada N, Yokomori H.** 2013. Relation between ultrastructural localization, changes in caveolin-1, and capillarization of liver sinusoidal endothelial cells in human hepatitis C-related cirrhotic liver. J Histochem Cytochem **61:**169–176. http://dx.doi.org/10.1369/0022155412468590.
35. **Neumann K, Erben U, Kruse N, Wechsung K, Schumann M, Klugewitz K, Scheffold A, Kühl AA.** 2015. Chemokine transfer by liver sinusoidal endothelial cells contributes to the recruitment of CD4+ T cells into the murine liver. PLoS One **10:**e0123867. http://dx.doi.org/10.1371/journal.pone.0123867.
36. **Pope M, Marsden PA, Cole E, Sloan S, Fung LS, Ning Q, Ding JW, Leibowitz JL, Phillips MJ, Levy GA.** 1998. Resistance to murine hepatitis virus strain 3 is dependent on production of nitric oxide. J Virol **72:**7084–7090.
37. **Iwakiri Y, Kim MY.** 2015. Nitric oxide in liver diseases. Trends Pharmacol Sci **36:**524–536. http://dx.doi.org/10.1016/j.tips.2015.05.001.
38. **Yokomori H, Oda M, Yoshimura K, Nomura M, Wakabayashi G, Kitajima M, Ishii H.** 2003. Elevated expression of caveolin-1 at protein and mRNA level in human cirrhotic liver: relation with nitric oxide. J Gastroenterol **38:**854–860. http://dx.doi.org/10.1007/s00535-003-1161-4.
39. **Peyrefitte CN, Pastorino B, Grau GE, Lou J, Tolou H, Couissinier-Paris P.** 2006. Dengue virus infection of human microvascular endothelial cells from different vascular beds promotes both common and specific functional changes. J Med Virol **78:**229–242. http://dx.doi.org/10.1002/jmv.20532.
40. **Connolly MK, Bedrosian AS, Malhotra A, Henning JR, Ibrahim J, Vera V, Cieza-Rubio NE, Hassan BU, Pachter HL, Cohen S, Frey AB, Miller G.** 2010. In hepatic fibrosis, liver sinusoidal endothelial cells acquire enhanced immunogenicity. J Immunol **185:**2200–2208. http://dx.doi.org/10.4049/jimmunol.1000332.
41. **Jacques A, Bleau C, Turbide C, Beauchemin N, Lamontagne L.** 2009. Macrophage interleukin-6 and tumour necrosis factor-alpha are induced by coronavirus fixation to Toll-like receptor 2/heparan sulphate receptors but not carcinoembryonic cell adhesion antigen 1a. Immunology **128:**e181–192. http://dx.doi.org/10.1111/j.1365-2567.2008.02946.x.
42. **Ganesan LP, Mohanty S, Kim J, Clark KR, Robinson JM, Anderson CL.** 2011. Rapid and efficient clearance of blood-borne virus by liver sinusoidal endothelium. PLoS Pathog **7:**e1002281. http://dx.doi.org/10.1371/journal.ppat.1002281.
43. **Simon-Santamaria J, Rinaldo CH, Kardas P, Li R, Malovic I, Elvevold K, McCourt P, Smedsrød B, Hirsch HH, Sørensen KK.** 2014. Efficient uptake of blood-borne BK and JC polyomavirus-like particles in endothelial cells of liver sinusoids and renal vasa recta. PLoS One **9:**e111762. http://dx.doi.org/10.1371/journal.pone.0111762.
44. **Carambia A, Frenzel C, Bruns OT, Schwinge D, Reimer R, Hohenberg H, Huber S, Tiegs G, Schramm C, Lohse AW, Herkel J.** 2013. Inhibition of inflammatory CD4 T cell activity by murine liver sinusoidal endothelial cells. J Hepatol **58:**112–118. http://dx.doi.org/10.1016/j.jhep.2012.09.008.
45. **Lamontagne L, Dupuy JM.** 1987. Characterization of a non pathogenic MHV3 variant derived from a persistently infected lymphoid cell line. Adv Exp Med Biol **218:**255–263. http://dx.doi.org/10.1007/978-1-4684-1280-2_30.
46. **Sutmuller RP, den Brok MH, Kramer M, Bennink EJ, Toonen LW, Kullberg BJ, Joosten LA, Akira S, Netea MG, Adema GJ.** 2006. Toll-like receptor 2 controls expansion and function of regulatory T cells. J Clin Invest **116:**485–494. http://dx.doi.org/10.1172/JCI25439.
47. **Liu G, Zhao Y.** 2007. Toll-like receptors and immune regulation: their direct and indirect modulation on regulatory CD4+ CD25+ T cells. Immunology **122:**149–156. http://dx.doi.org/10.1111/j.1365-2567.2007.02651.x.
48. **Banerjee S, Narayanan K, Mizutani T, Makino S.** 2002. Murine coronavirus replication-induced p38 mitogen-activated protein kinase activation promotes interleukin-6 production and virus replication in cultured cells. J Virol **76:**5937–5948. http://dx.doi.org/10.1128/JVI.76.12.5937-5948.2002.
49. **Lamontagne L, Descoteaux JP, Jolicoeur P.** 1989. Mouse hepatitis virus 3 replication in T and B lymphocytes correlate with viral pathogenicity. J Immunol **142:**4458–4465.
50. **Tsuhako MH, Augusto O, Linares E, Dagli ML, Pereira CA.** 2006. Association between nitric oxide synthesis and vaccination-acquired resistance to murine hepatitis virus by SPF mice. Free Radic Biol Med **41:**1534–1541. http://dx.doi.org/10.1016/j.freeradbiomed.2006.08.011.
51. **Ning Q, Liu M, Kongkham P, Lai MM, Marsden PA, Tseng J, Pereira B, Belyavskyi M, Leibowitz J, Phillips MJ, Levy G.** 1999. The nucleocapsid protein of murine hepatitis virus type 3 induces transcription of the novel fgl2 prothrombinase gene. J Biol Chem **274:**9930–9936. http://dx.doi.org/10.1074/jbc.274.15.9930.
52. **Liu J, Tan Y, Zhang J, Zou L, Deng G, Xu X, Wang F, Ma Z, Zhang J, Zhao T, Liu Y, Li Y, Zhu B, Guo B.** 2015. C5aR, TNF-α, and FGL2 contribute to coagulation and complement activation in virus-induced fulminant hepatitis. J Hepatol **62:**354–362. http://dx.doi.org/10.1016/j.jhep.2014.08.050.
53. **Arshad MI, Piquet-Pellorce C, Samson M.** 2012. IL-33 and HMGB1 alarmins: sensors of cellular death and their involvement in liver pathology. Liver Int **32:**1200–1210. http://dx.doi.org/10.1111/j.1478-3231.2012.02802.x.
54. **Wang J, Zhao P, Guo H, Sun X, Jiang Z, Xu L, Feng J, Niu J, Jiang Y.** 2012. Serum IL-33 levels are associated with liver damage in patients with chronic hepatitis C. Mediat Inflam **2012:**819636.
55. **Wang J, Cai Y, Ji H, Feng J, Ayana DA, Niu J, Jiang Y.** 2012. Serum IL-33 levels are associated with liver damage in patients with chronic hepatitis B. J Interferon Cytokine Res **32:**248–253. http://dx.doi.org/10.1089/jir.2011.0109.
56. **Pircher J, Czermak T, Merkle M, Mannell H, Krötz F, Ribeiro A, Vielhauer V, Nadjiri J, Gaitzsch E, Niemeyer M, Porubsky S, Gröne HJ, Wörnle M.** 2014. Hepatitis C virus induced endothelial inflammatory response depends on the functional expression of TNFα receptor subtype 2. PLoS One **9:**e113351. http://dx.doi.org/10.1371/journal.pone.0113351.

57. **Cooper A, Tal G, Lider O, Shaul Y.** 2005. Cytokine induction by the hepatitis B virus capsid in macrophages is facilitated by membrane heparan sulfate and involves TLR2. J Immunol **175:**3165–3176. http://dx.doi.org/10.4049/jimmunol.175.5.3165.
58. **Dolganiuc A, Oak S, Kodys K, Golenbock DT, Finberg RW, Kurt-Jones E, Szabo G.** 2004. Hepatitis C core and nonstructural 3 proteins trigger Toll-like receptor 2-mediated pathways and inflammatory activation. Gastroenterology **127:**1513–1524. http://dx.doi.org/10.1053/j.gastro.2004.08.067.
59. **Berzsenyi MD, Roberts SK, Preiss S, Woollard DJ, Beard MR, Skinner NA, Bowden DS, Visvanathan K.** 2011. Hepatic TLR2 and TLR4 expression correlates with hepatic inflammation and TNF-α in HCV and HCV/HIV infection. J Viral Hepat **18:**852–860. http://dx.doi.org/10.1111/j.1365-2893.2010.01390.x.